

Regulation of retinal axon growth by secreted Vax1 homeodomain protein

Namsuk Kim¹, Kwang Wook Min¹, Kyung Hwa Kang², Eun Jung Lee¹, Hyung-Tai Kim¹,
Kyunghwan Moon¹, Jiheon Choi¹, Dai Le¹, Sang-Hee Lee¹, and Jin Woo Kim^{1,2,3}

¹Department of Biological Sciences; ²KAIST Institute of BioCentury, Korea Advanced
Institute of Science and Technology (KAIST), Daejeon 305-701, South Korea

³Correspondence to: jinwookim@kaist.ac.kr

Abstract

Retinal ganglion cell (RGC) axons of binocular animals cross the midline at the optic chiasm (OC) to grow toward their synaptic targets in the contralateral brain. Ventral anterior homeobox 1 (Vax1) plays an essential role in the development of the OC by regulating RGC axon growth in a non-cell autonomous manner. Here, we identify an unexpected function of Vax1 that is secreted from ventral hypothalamic cells and diffuses to RGC axons, where it promotes axonal growth independent of its transcription factor activity. We demonstrate that Vax1 binds to extracellular sugar groups of the heparan sulfate proteoglycans (HSPGs) located in RGC axons. Both Vax1 binding to HSPGs and subsequent penetration into the axoplasm, where Vax1 activates local protein synthesis, are required for RGC axonal growth. Together, our findings demonstrate that Vax1 possesses a novel RGC axon growth factor activity that is critical for the development of the mammalian binocular visual system.

Introduction

Development of the mammalian binocular visual system requires topographic synaptic connections of retinal ganglion cell (RGC) axons to neurons on the lateral geniculate nucleus and superior colliculus of the brain (Lemke & Reber, 2005). To access their synaptic targets, RGC axons exit from the retina and grow in selective directions by recognizing guidance cues expressed in optic pathway structures, including the optic disc (OD), optic stalk (OS), optic chiasm (OC), and optic tract (OT) (Petros et al, 2008). RGC axon guidance cues include cell surface ligands such as semaphorins in the OS and ephrinB2 in the OC, and soluble factors such as netrin-1 in the OD and Slit1 in areas surrounding the OC (Erskine & Herrera, 2007). Ultimately, only about 3% of mouse RGC axons, which originate from the ventral and temporal part of retina, are linked to targets on the same side of brain, whereas a majority of RGC axons are connected to those on the opposite side after crossing the midline at the OC, located at the ventral-medial hypothalamic (vHT) area.

Subsets of vHT cells therefore express molecules that determine the directionalities of RGC axons at the OC. It has been shown that vHT radial glial cells express ephrinB2, which binds to EphB1 receptors expressed in ventral-temporal RGC axons and repels the axons toward the ipsilateral optic tract (Nakagawa et al, 2000; Williams et al, 2003). In

addition, vascular endothelial growth factor 164 (VEGF164), an isoform of the vascular endothelial growth factor VEGF-A (Soker et al, 1996), and neuronal cell adhesion molecule (NrCAM) expressed in the vHT have been suggested to support the growth of RGC axons across the vHT midline by binding to neuropilin 1 and plexin A1, respectively (Erskine et al, 2011; Kuwajima et al, 2012; Williams et al, 2006). To receive the directional guidance of these molecules at the vHT, RGC axons must pass through the ventral-lateral diencephalic area, where repulsive guidance cues, such as Slit and semaphorins, are expressed at high levels (Erskine et al, 2000; Plump et al, 2002). However, the molecules that support RGC axon growth toward the vHT midline are still unknown.

Ventral anterior homeobox 1 (*Vax1*) is a homeodomain transcription factor expressed in various ventral-medial forebrain-derived structures, including the medial and lateral geniculate eminences, the ventral septum, the anterior entopeduncular area, the preoptic area, the vHT, and the OS (Bertuzzi et al, 1999; Hallonet et al, 1998). Genetic inactivation of *Vax1* in humans and mice causes agenesis of multiple midline structures of the brain, including the anterior commissure, the corpus callosum and the OC, in addition to the coloboma of the eye (Bertuzzi et al, 1999; Hallonet et al, 1999; Slavotinek et al, 2012). RGC axons in *Vax1*-deficient mice can grow through the OS, but cannot access the vHT area and fail to form an OC. *Vax1* is not expressed in RGCs despite its critical roles in growth and fasciculation of RGC axons (Bertuzzi et al, 1999; Mui et al, 2005). Therefore, it has been suggested that defects in OC formation in *Vax1*-deficient mouse RGCs might be caused by the loss or gain of axon guidance cues that are potential transcription targets of *Vax1* in vHT cells.

Contrary to expectation, we here found that *Vax1* promoted RGC axon growth in a transcription-independent manner. Moreover, *Vax1* is secreted from vHT cells and binds and enters RGC axons to stimulate axonal growth. This unexpected trafficking of *Vax1* to RGC axons was mediated by heparan sulfate proteoglycans (HSPGs), such as syndecan and glypican, expressed in RGC axons. However, *Vax1* binding to HSPGs was not sufficient to trigger RGC axon growth; penetration into the RGC axoplasm and subsequent stimulation of local protein synthesis were also necessary. Taken together, our findings reveal an unconventional function of *Vax1* as an RGC axon growth factor that enables RGC axons to grow toward the midline during development.

Results

Vax1 regulates RGC axonal growth in a non-cell autonomous manner

Vax1 is expressed in cells located in optic pathway structures, such as the OS and vHT, and plays an essential role in fasciculation of RGC axons and formation of the OC (Bertuzzi et al, 1999; Hallonet et al, 1999). At the vHT of days post coitum 14.5 (E14.5) mouse embryo, *Vax1* is expressed in Sox2 (SRY box 2)-positive neural progenitor cells (NPCs) and RC2-detectable nestin-positive radial glia (Figure 1A,B; top rows), which are known to provide RGC axon guidance cues (Petros et al, 2008). Although the morphology of the chiasm is abnormal in *Vax1*-deficient (*Vax1*^{-/-}) mice (Bertuzzi et al, 1999), these OC-forming cells and several chiasm-localized cues (NrCAM and Vegfa) are still present (Figure 1A,B [bottom rows]; Figure 1 – figure supplement 1). However, vHT explants from *Vax1*^{-/-} mice were unable to attract RGC axons regardless of the *Vax1* gene status of co-cultured retinal explants, whereas wild-type (WT) vHT explants were able to attract RGC axons projected from *Vax1*^{-/-} explants as well as WT explants (Figure 1C,D). We therefore concluded that *Vax1* controls RGC axonal growth in a non-cell autonomous manner, potentially by regulating the expression of unidentified secreted axon-guidance molecules.

Vax1 is a secreted protein

To identify *Vax1*-regulated secreted factors that control RGC axonal growth from co-cultured retinal explants, we overexpressed mouse *Vax1* in COS7 cells. RGC axons from retinal explants grew preferentially toward co-cultured *Vax1*-expressing COS7 cell aggregates, whereas RGC axons projected in random directions upon co-incubation with untransfected or *Vax2*-overexpressing COS7 cell aggregates (Figure 2A,B). Because *Vax2* shares an identical homeodomain with *Vax1* (Barbieri et al, 1999), these results indicate that the RGC axon growth-stimulatory activity is specific for *Vax1*.

We next examined whether *Vax1*-induced RGC axonal growth is dependent on *Vax1* transcription activity by co-incubating retinal explants with COS7 cells expressing a transcriptionally inactive *Vax1*(R152S) mutant (Figure 2; Figure 2 – figure supplement 1). This mutation was reported in human patients that exhibit coloboma, cleft palate and agenesis of corpus callosum (ACC), phenotypic manifestations similar to those of *Vax1*-deficient mice (Slavotinek et al, 2012). Unexpectedly, we found that *Vax1*(R152S)-expressing COS7 cells were also able to induce RGC axonal growth as efficiently as WT

Vax1-expressing COS7 cells (Figure 2A[third row], B), suggesting that Vax1 induces RGC axonal growth in a transcription-independent manner.

More strikingly, Vax1 and Vax1(R152S) proteins were not only expressed in transfected COS7 cells, they were also detectable in neurofilament 160 kDa (NF160)-positive RGC axons projecting from co-cultured retinal explants (Figure 2A, right two columns). These axonal Vax1 immunostaining signals were remarkably decreased in the presence of a rabbit anti-Vax1 polyclonal antibody (α -Vax1) that sequesters Vax1 in the growth medium (Figure 2 – figure supplement 2). Furthermore, Vax1 and Vax1(R152S) proteins were found in the growth medium of transfected COS7 cells, whereas Vax2 protein was not (Figure 2C). Since the viability of the transfected COS7 cells were not different from each other (data not shown), these results suggest that Vax1 proteins in the growth medium and co-cultured RGC axons did not originate from dead cells. Similar to overexpressed Vax1 in COS7 cells, endogenous Vax1 expressed in vHT explants was detectable in the growth medium (Figure 2D). Furthermore, Vax1 protein was also identified in the cerebral spinal fluid (CSF) of E14.5 mouse embryos (Figure 2E), suggesting that Vax1 is secreted *in vivo* as well as *in vitro*.

Vax1 has retinal axon growth factor activity

We further tested whether secreted Vax1 is capable of directly binding to RGC axons and regulating axonal growth using purified recombinant Vax1 protein. Time-lapse recordings of RGC axons revealed that fluorescein isothiocyanate (FITC)-labeled, His-tagged Vax1 (Vax1-His) protein added to the growth medium of retinal explants accumulated in RGC axons and exerted strong growth stimulatory effects on them (Figure 3A,B; Video supplements 1 and 2; Figure 3 – figure supplement 1). The axon growth stimulating effects of Vax1-His were applied equally to retinal quadrants (Figure 3 – figure supplement 2), implicating Vax1 is not a region-specific axon growth factor. The transcriptionally inactive Vax1(R152S)-His mutant protein was also detectable in RGC axons and stimulated axonal growth as efficiently as WT Vax1-His (Figure 3C,D), suggesting that extracellular Vax1 moves to RGC axons and induces axonal growth in transcription-independent manner. Despite that Vax2 is not secreted (Figure 2C), the ability of recombinant Vax2-His to be internalized and induce RGC axonal growth is almost equivalent to that of Vax1 (Figure 3 – figure supplement 3), implicating that internalization but not secretion is a conserved characteristic of VAX transcription factors.

In vivo evidence for intercellular transfer of Vax1

We next sought evidence for transfer of Vax1 to RGC axons *in vivo*. As reported previously (Bertuzzi et al, 1999; Hallonet et al, 1998), *Vax1* mRNA is expressed in RGC axon-associated structures, including the OD, the OS, and the vHT, but not the retina, of E14.5 mice (Figure 4A; Figure 4 – figure supplement 1A). However, an examination of *Vax1* protein distribution in E14.5 *Vax1^{lacZ/+}* heterozygous mouse embryos showed that *Vax1* was detectable in the retina as well as the OS and OD (Figure 4B, top row). In these mice, β -galactosidase (β -gal) is expressed from a *lacZ* gene replacing one *Vax1* gene locus while *Vax1* is expressed from the other intact *Vax1* gene locus (Hallonet et al, 1999); therefore, β -gal should be expressed in cells expressing *Vax1*. However, we found that RGCs in *Vax1^{lacZ/+}* mice did not express β -gal, but did express *Vax1*; this contrasts with OS APCs, which co-expressed *Vax1* and β -gal (Figure 4B, top row). *Vax1* immunostaining signals were completely absent in RGCs as well as β -gal-positive OS APCs from homozygous *lacZ* knock-in *Vax1^{lacZ/lacZ}* littermates, suggesting that *Vax1* immunostaining signals in the *Vax1^{lacZ/+}* mouse RGC were specific (Figure 4B, bottom row). Collectively, these data demonstrate that *Vax1* protein in RGCs might originate from neighboring *Vax1*/ β -gal double-positive APCs in the OS or NPCs and radial glia in the vHT (Figure 4B; Figure 4 – figure supplement 1B).

Vax1 protein in OS APCs was present mainly in nuclei, whereas a majority of *Vax1* protein in β -gal-negative RGCs was non-nuclear (Figure 4B, i and ii). Furthermore, *Vax1* co-localized with NF160 in E14.5 WT mouse RGC axons, but was lost in *Vax1^{lacZ/lacZ}* mouse RGC axons (Figure 4C). These *Vax1* localization patterns in OS APCs and RGCs were further confirmed by immuno-transmission electron microscopy. *Vax1* protein was highly enriched at the extracellular part of the RGC membrane, and was also detected in the cytoplasm and intracellular vesicles (Figure 4D, top row; Figure 4 – figure supplement 2). *Vax1* protein in OS APCs was not only enriched in nuclei, but was also detectable in cytoplasmic membrane structures (Figure 4D, bottom row). These results therefore suggest that OS- and/or vHT-secreted *Vax1* might enter RGCs after docking with the RGC axon membrane.

Intercellular transfer of Vax1 is necessary for RGC axonal growth

To investigate whether secreted Vax1 is necessary for the growth of RGC axons toward vHT explants, we sequestered extracellular Vax1 using α -Vax1. α -Vax1 not only interfered with the transfer of Vax1 from vHT cells to RGC axons, it also antagonized RGC axonal growth toward vHT explants (Figure 5A, center). In contrast, neither rb-IgG (pre-immune rabbit IgG) nor α -Vax2 influenced Vax1 transfer into RGC axons or RGC axonal growth toward vHT explants (Figure 5A, left and right). α -Vax1 treatment not only reduced the population of retinal axons growing toward the vHT (Figure 5B), it also decreased the total number of retinal axons growing from the explants (Figure 5C), suggesting an axogenic activity as well as an axon growth-stimulating activity of extracellular Vax1.

The roles of extracellular Vax1 in RGC axon growth were also investigated *in vivo*. Collagen gels releasing rb-IgG or α -Vax1 were implanted in the third ventricle of E13.5 mouse embryonic brain slabs to sequester extracellular Vax1 in the vHT area (Figure 5D, diagram on top panel). Mouse embryos implanted with α -Vax1–releasing gels showed a remarkable reduction in RGC axons accessing the midline compared with embryos implanted with rb-IgG–releasing gels (Figure 5D). In α -Vax1–implanted mouse embryos, a significant number of RGC axons showed reduced Vax1 immunoreactivity and stopped at the lateral wall of the ventral diencephalon, properties similar to those observed in *Vax1*-deficient mice (Bertuzzi et al, 1999) (Figure 5D, bottom row). Taken together, these results suggest that extracellular Vax1 is necessary for RGC axonal growth to the ventral midline.

Heparan sulfate proteoglycan regulates Vax1 intercellular transfer

Intercellular transfer has also been reported for other homeodomain transcription factors, such as engrailed-2 (En2) and orthodenticle homeobox 2 (Otx2) (Joliot et al, 1998; Spatazza et al, 2013; Sugiyama et al, 2008). However, little is known about the regulatory mechanisms underlying the trafficking of homeodomain transcription factors. We therefore searched for genes encoding proteins capable of modifying the intercellular transfer of Vax1 in *Drosophila* (Figure 6; *screening results are unpublished*). One of the genes isolated in this screen encodes the transmembrane heparan sulfate proteoglycan (HSPG) protein, syndecan (Sdc) (Spring et al, 1994). HSPGs, including Sdc2, Sdc3 and glypican 1 (Glp1), are highly expressed in mouse RGC axons and have been proposed to play critical roles in RGC axon guidance in various vertebrates (Chung et al, 2001; Inatani et al, 2003; Lee & Chien, 2004; Pratt et al, 2006). We thus focused on the potential role of HSPGs as receptors for Vax1 in RGC axons.

Vax1-GFP protein was co-expressed with DsRed protein in A/P (anterior/posterior) boundary cells of *Drosophila* wing imaginal disc under the control of a *Ptc-Gal4* driver. Vax1-GFP, but not DsRed, was transferred to neighboring cells, results similar to those observed in mammalian systems (Figure 6, top row). However, the transfer of Vax1-GFP to neighboring wing disc cells was suppressed upon co-expression of Sdc in A/P boundary cells (Figure 6, third row). Overexpressed dally-like protein (Dlp), a *Drosophila* homolog of Glp, also suppressed Vax1 transfer in the same manner as Sdc (Figure 6, bottom row), suggesting that the intercellular transfer of Vax1 in *Drosophila* wing imaginal disc cells is mediated by HSPGs but not specifically by Sdc. These results also imply that these overexpressed HSPGs in A/P boundary cells captured co-expressed Vax1-GFP protein, thereby interfering with the transfer of Vax1-GFP to neighboring cells (Figure 6, diagram in right column). Conversely, Vax1-GFP proteins were transferred farther in *Sdc* mutant (*Sdc*²³) wing imaginal disc, where total HSPG levels were reduced owing to the loss of Sdc (Figure 6, second row).

Heparan sulfate-dependent binding of Vax1 to HSPGs is required for Vax1-induced RGC axonal growth

HSPG-regulated Vax1 transfer was further investigated in mammalian systems. We found that Vax1, but not Vax2, interacted with Sdc2 in E14.5 mouse optic nerves as well as with overexpressed Sdc1 and Sdc2 in human embryonic kidney (HEK) 293T cells (Figure 7A, Figure 7 – figure supplement 1A,B). Sdc2-N, lacking the C-terminal cytoplasmic domain, was able to interact with Vax1, whereas Sdc2-C, which lacks the N-terminal extracellular domain, failed to interact with Vax1 (Figure 7 – figure supplement 1C), suggesting that Vax1 binds to the extracellular domain of Sdc.

The extracellular domain of Sdc is attached by heparan sulfate (HS) sugars (Bishop et al, 2007); thus, Vax1 could interact with the sugar groups as well as the protein backbone of Sdc. To determine the potential binding of Vax1 to HS side chains of Sdc2 in RGC axons, we used co-immunoprecipitation assays to test whether excess free heparin competed with HS side chains of HSPGs, including Sdc2, Sdc3 and Glp1, for binding to Vax1. Vax1 interactions with each of these HSPGs expressed in RGC axons in E14.5 optic nerves were disrupted in the presence of free heparin, whereas interactions with Pax2 (paired homeobox 2), which complexes with Vax1 in OS APCs, were not (Figure 7B). Moreover, recombinant Vax1-His specifically bound HS-Sepharose resin with high affinity

(Figure 7C). Collectively, these results suggest that Vax1 preferentially binds to HS side chains of HSPG proteins expressed in RGC axons.

We also examined the influence of Vax1 binding to HSPGs on RGC axon growth. Sdc3 was expressed in E14.5 mouse RGCs in a non-polarized manner and co-localized with Vax1 in RGC axons (Figure 7 – figure supplement 2). The growth-stimulatory effects of Vax1 on RGC axons were abolished by treatment of retinal explants with heparinase I, which cleaves heparin and HS sugar chains, but not by incubation with chondroitinase ABC (ChnaseABC), which digests chondroitin sugar chains (Bishop et al, 2007) (Figure 7D,E). Heparinase I treatment also decreased the immunostaining intensity of exogenously provided Vax1-His in RGC axons (Figure 7D). Neither heparinase I nor ChnaseABC influenced RGC axon growth in the absence of Vax1 (Figure 7D,E). Collectively, these results suggest that the binding of Vax1 to HSPGs is necessary for the induction of RGC axonal growth.

Vax1-induced RGC growth requires local protein synthesis

Secreted Vax1 not only bound to HSPGs at the RGC cell surface, it also moved into the RGC axoplasm by exploiting the cell-penetrating property of its homeodomain (Joliot & Prochiantz, 2004) (Figure 4D; Figure 4 – figure supplement 2). It is therefore possible that Vax1 stimulates RGC axonal growth either by acting as a ligand for HSPGs or by regulating cytoplasmic events after penetration. To answer this question, we tested the function of a Vax1(WF/SR) mutant, in which conserved Trp147 and Phe148 amino acids responsible for cell penetration were replaced with Ser167 and Arg148 (Joliot et al, 1998); this mutant lacks the ability to cross the cell membrane but remains capable of binding to Sdc2 (Figure 8 – figure supplement 1A,B). We found that Vax1(WF/SR) barely penetrated RGC axons and induced RGC axonal growth less efficiently than WT Vax1 (Figure 8 – figure supplement 1C,D). These results suggest that Vax1-induced RGC axonal growth requires cell penetration.

To determine which cytoplasmic events Vax1 might affect, we identified cytoplasmic Vax1-interacting proteins by MALDI-TOF (matrix-assisted laser desorption/ionization-time of flight) mass spectrometry (Figure 8A). Interestingly, a majority of proteins isolated by Vax1-affinity purification were related to protein synthesis, including ribosomal proteins (RPs) L11, L23A, L26, S14, and S16; translation regulators, such as eukaryotic translation initiation factor (eIF) 3B and 3C; and the chaperone HSPA1A (heat shock 70-kDa protein 1A). These data suggest that Vax1 might act in RGC axons by modulating protein

synthesis, a mechanism similar to that by which cytoplasmic En2 controls RGC axonal growth (Brunet et al, 2005; Yoon et al, 2012). To confirm this, we tested the effects of Vax1 on protein synthesis in RGC axons by quantifying newly synthesized proteins, measuring the fluorescence intensity of incorporated bioorthogonal noncanonical amino acid azidohomoalanine (AHA), labeled with Alexa Fluor 488 by click chemistry (Dieterich et al, 2007). Treatment with Vax1-His induced a remarkable increase in the fluorescence intensities of AHA-Fluor 488-labeled proteins in RGC axons (Figure 8B, middle column), whereas the Vax1(WF/SR)-His had no effect on protein synthesis (Figure 8B, right column), indicating that intracellular Vax1 stimulated protein synthesis.

In contrast to its significant induction of protein synthesis in axons, Vax1-His–induced effects on AHA-Fluor 488 fluorescence intensities in retinal cell bodies were not notably different from those of Vax1(WF/SR)-His or the 6X-His peptide (Figure 8B, bottom row). Similarly, Vax1 failed to stimulate general translation in cultured cell-lines and purified polysomes *in vitro* (data not shown). In contrast, isolated retinal axons from the cell body still responded to Vax1 as efficiently as those that projected from intact retinal explants (Figure 8C,D). Taken together, these results suggest that Vax1 stimulates RGC axon growth by stimulating local translation of specific mRNA in the axon rather than by modulating gene expression in the cell body.

Imported Vax1 promotes the access of RGC axons to the midline

We further investigated whether extracellular Vax1 could restore RGC axon growth toward the midline in *Vax1*^{-/-} mice by re-supplying Vax1 protein to the vHT extracellular space. In contrast to the lack of RGC axon access to the vHT observed in *Vax1*^{-/-} mouse embryos, remarkable numbers of RGC axons were detectable in the vHT of *Vax1*^{-/-} mouse embryos implanted with collagen gels that released recombinant Vax1-His (Figure 9A[top rows of left two columns], B). Remarkable numbers of RGC axons were able to grow to the source of extracellular Vax1 protein (i.e., the third ventricle), although they failed to restore the OC. In contrast, implantation of collagen gels that released cell-penetration–defective Vax1(WF/SR)-His did not induce regrowth of RGC axons (Figure 9A[third column], B). Implanted recombinant Vax1-His was detectable in RGC axons, whereas Vax1(WF/SR)-His was not, suggesting that implanted Vax1 stimulated RGC axon growth by penetrating into the axoplasm.

It has been suggested that the avoidance of RGC axons in *Vax1*-deficient mouse vHT might result from high concentrations of Slit protein in the ventral lateral diencephalon

(Bertuzzi et al, 1999). In support of this, the growth of RGC axons toward *Vax1*-ko vHT explants were partly recovered by sequestering extracellular Slit protein using an Fc-fused extracellular fragment of the Slit receptor Robo1 (Robo1-Fc) (Figure 9 – figure supplement 1). Thus, we further investigated the roles of Slit in RGC axon avoidance in *Vax1*-deficient mouse embryos using Robo1-Fc. The growth of RGC axons into the vHT was partially rescued by implanting a Robo1-Fc–releasing collagen gel into the third ventricle, an effect that was further enhanced by implantation of gels co-releasing Vax1-His and Robo1-Fc (Figure 9A[two right columns], B).

Discussion

RGC axonal projection to the OC is often compared to spinal commissural axonal projection toward the floor plate (FP). Spinal commissural axons are prevented from prematurely entering the midline by Slit1 expressed in the medial spinal cord and grow in the ventral direction (Stein & Tessier-Lavigne, 2001). In much the same way, Slit1 in the preoptic area and ventral-lateral diencephalon prevents RGC axons from accessing the brain anywhere but at the vHT to form the OC (Erskine et al, 2000; Plump et al, 2002). The spinal commissural axons sense attractive cues, such as netrin and Shh, secreted from the FP (Charron et al, 2003; Stein & Tessier-Lavigne, 2001). The attractive netrin and Shh signals are expected to compete with the coexisting repulsive signal of Slit2, which can be accumulated locally by HSPGs, including α -dystroglycan, at the ventral FP (vFP), to determine the directionality of spinal commissural axon growth cones (Matsumoto et al, 2007; Wright et al, 2012). RGC-expressed HSPGs were also reported to play roles as co-receptors for netrin and Slit (Hussain et al, 2006; Johnson et al, 2004; Ogata-Iwao et al, 2011), suggesting a similar HSPG-based antagonistic regulation of RGC axon growth. However, both netrin and Shh are dispensable with respect to attracting RGC axons toward the vHT, and instead function as repulsive cues for RGC axons (Deiner & Sretavan, 1999; Sanchez-Camacho & Bovolenta, 2008). In this study, we propose vHT-secreted Vax1 as a RGC axon growth factor that is analogous to vFP-secreted netrin and Shh. This unconventional axon growth factor also utilizes HSPGs for anchoring to RGC axons (Figure 7) and could compete with Slit for HSPGs binding *in vitro* (Figure 9 – figure supplement 2). However, it is unclear whether this competition is valid in physiological conditions, because Slit does not inhibit RGC axon growth toward the vHT midline

(Erskine et al, 2000; Plump et al, 2002). Moreover, cell penetration-defective Vax1(WF/SR) mutant could not induce RGC axon growth *in vivo* as well as *in vitro*, despite of its capability of HSPG binding (Figure 8,9; Figure 8 – figure supplement 1). It suggests that HSPG binding of Vax1 is not sufficient to induce RGC axon growth, but local protein synthesis induced by internalized Vax1 is necessary. Collectively, we propose a hypothetical model that Vax1 promotes RGC axon growth toward the vHT midline by directly targeting mRNA in the axons rather than by serving for a conventional axon guidance molecule that binds specific receptors and triggers on intracellular signaling cascades (Figure 10). Identification of axonal target mRNA awaits future investigations.

Translation-dependent, but transcription-independent, RGC axon guidance by a secreted transcription factor has also been reported for En2, which regulates RGC growth cone turning by increasing the expression of mitochondrial proteins involved in elevating local ATP, which potentiates ephrin-A5 signaling (Brunet et al, 2005; Stettler et al, 2012; Yoon et al, 2012). Since Vax1 and En2 share a homologous homeodomain, Vax1 could function in a similar manner by cooperating with attractive RGC axon guidance cues, such as VEGF164 and NrCAM (Erskine et al, 2011; Kuwajima et al, 2012; Williams et al, 2006), by modulating mitochondrial activity. Conversely, En2 could also use HSPGs to bind target axons and fine-tune their selective growth.

In their use of HSPGs as docking sites for RGC axons, Vax1 can be compared to Otx2, which binds specifically to CSPGs of the perineuronal net surrounding parvalbumin (PV) neurons in visual cortex (Beurdeley et al, 2012; Miyata et al, 2012). The differential affinities of Vax1 and Otx2 for HS and CS might be related to their different homeodomains. Among homeodomain proteins proven to exhibit transfer, Vax1 possesses an antennapedia class homeodomain homologous to that of Emx2 and En2, whereas Otx2 shares a paired class homeodomain similar to that of Pax6 (paired box 6) (Bürglin, 2011; Spatazza et al, 2013). One intriguing possibility that has not yet been explored is that these secreted homeodomain proteins share the property of preferential binding to HS and CS; however, it is at least as likely that intercellular transfer of homeodomain proteins are target-selective events.

Vax2 was not as effectively secreted from COS7 cells as Vax1 (Figure 2), despite sharing an identical homeodomain with Vax1. This suggests that secretion of Vax1 is not solely mediated by the homeodomain but is also dependent on a three-dimensional structure that supports the secretion property of the homeodomain. Unlike Vax1, Vax2 undergoes a specific phosphorylation that results in its cytoplasmic retention (Kim &

Lemke, 2006). Phosphorylation of En2 inhibits its secretion (Maizel et al, 2002), suggesting that phosphorylation might change the structure of these proteins in such a way that it interferes with homeodomain recognition by secretion regulators. However, phosphorylation-defective Vax1(S170A) was still unable to be secreted from COS7 cells (data not shown). Instead, Vax2 could be secreted from different types of cells, where Vax2 might form three-dimensional structures that can be recognizable by secretion machineries (Lee et al., unpublished data). The results suggest that secretion of homeodomain proteins is a cell context-dependent event.

Multiple midline-crossing defects, including agenesis of the corpus callosum, anterior commissure and hippocampal commissure, are observed in *Vax1*-deficient mice and homozygous *VAX1* mutant human patients (Bertuzzi et al, 1999; Slavotinek et al, 2012). However, the molecular functions of Vax1 in the development of these structures remain unknown. In this study, we show that Vax1-induced RGC axonal growth is independent of its transcription factor activity (Figure 2A and 3C). Instead, Vax1 acts as a regulator of translation after penetrating into RGC axons (Figure 8). Although we cannot rule out Vax1 functions as a transcription factor in the development of those commissures, our results suggest a potential role of secreted Vax1 in the growth of cortical axons (Min et al., unpublished data). Whether axonal growth of these commissural axons in the mammalian forebrain also requires local protein synthesis triggered by Vax1 protein secreted from cells located in other midline structures, such as the ventral-medial telencephalon and the septum, is a question that warrants further investigation.

Materials and Methods

Mice and explant culture

Vax1 knock-out (*Vax1*^{-/-}) and *Vax1* knock-in (*Vax1*^{lacZ/lacZ}) mice were reported previously (Bertuzzi et al, 1999; Hallonet et al, 1999). Retinal and vHT explants were cultured as described previously (Sato et al, 1994). Briefly, retinal or vHT explants were added to a collagen mixture and positioned on plates coated with poly-L-lysine (10 µg/ml) and laminin (10 µg/ml). The explants were then incubated at 37°C for 1 h to allow gelling before adding Neurobasal medium containing B27 supplement (Invitrogen). COS7 cell droplets (10⁵ cells/droplet) were also prepared using the same procedures. The explants were cultured

alone or co-cultured with vHT or COS7 explants for 48 h before treating with proteins and antibodies.

For time-lapse recording of retinal axon growth, mouse retinal explants were treated with FITC-labeled 6X-His peptide (100 ng/ml) or Vax1-His protein (500 ng/ml) for 24 h and photographed every 15 min using a Zeiss Axio Observer Z1 inverted microscope. The explants were washed twice with phosphate-buffered saline (PBS) prior to incubation with rabbit anti-Vax1 polyclonal antibody (α -Vax1; 1:100) for 30 min to detect Vax1-His located on the cell surface. The explants were then washed with PBS and fixed in 4% paraformaldehyde (PFA)/PBS for subsequent immunostaining procedures to detect total Vax1 protein inside and outside of cells.

For slab embryo culture with collagen gel implantation, E13.5 mouse embryos were moved onto culture slide chambers containing collagen mixture, positioning the dorsal part on top, after dissecting out the dorsal half of the brain and lower part of the mouth. Droplets of collagen solution mixed with pre-immune IgG (1 μ g/ml), α -Vax1 (1 μ g/ml), 6X-His peptide (4.78 μ g/ml), or Vax1-His (200 μ g/ml) protein was then delivered into the third ventricle of the slab embryos. The embryos were then filled with culture medium and incubated for 12 h at 37°C in a humidified atmosphere supplemented with 7% CO₂. The embryos were fixed in 4% PFA/PBS for subsequent freezing in OCT (optimal cutting temperature) medium. RGC axon growth at the vHT was monitored along the horizontal axis of slide-mounted embryonic brain sections under an Olympus BX-71 fluorescence microscope. The slides were then stained with appropriate antibodies and examined under an Olympus FV1000 confocal microscope to detect penetration of implanted Vax1 protein into RGC axons.

Retinal axon count

Relative axon counts (combined values of numbers and lengths of axons) of retinal explants were obtained by measuring NF160-fluorescent pixels in images of retinal axons using Image-J software. Relative axon counts of retinal explants co-cultured with vHT explants or COS7 cell aggregates were obtained along three angle segments: forward (+), neutral (0), and reverse (-). A clockwise angle from a line connecting two centers of explants was obtained and classified as forward direction (+) if it was between 0° and 60° or between 301° and 360°; neutral direction (0) if it was between 61° and 120° or between 241° and 300°; and reverse direction (-) if it was between 121° and 240° (Figure 2B and

5B). Relative axon counts in each angle segment was then obtained by comparing pixel counts of NF160 immunofluorescence in RGC axons of the explants in each angle segment.

Antibodies

α -Vax1 and α -Vax2 were produced as reported previously (Mui et al, 2005). Commercially available antibodies against the following proteins were used: mouse anti-Myc (Santa Cruz Biotechnology), mouse anti-GFP (Santa Cruz Biotechnology), mouse anti-tubulin β -III (Tuj1; Covance), goat anti-Sox2 (Santa Cruz Biotechnology), mouse anti-Nestin (RC2; Millipore), mouse anti- β -galactosidase (Developmental Studies Hybridoma Bank, DSHB), mouse anti-NF160 (Developmental Studies Hybridoma Bank (DSHB)), goat anti-Sdc2 (Santa Cruz Biotechnology), goat anti-Sdc3 (Santa Cruz Biotechnology; for immunohistochemistry), rabbit anti-Sdc3 (Abcam; for Western blot), rabbit anti-Glp1 (Santa Cruz Biotechnology), and rabbit anti-Pax2 (Invitrogen) antibodies.

Immunohistochemistry

The heads of embryonic mice were fixed in 4% PFA/PBS at 4°C for 2–16 h, depending on the protein to be detected, and then incubated in a 20% sucrose/PBS solution at 4°C for 16 h before embedding in OCT medium for freezing. Sections of frozen tissue were incubated for 1 h in a blocking solution containing 0.2% Triton X-100, 5% normal donkey serum, and 2% bovine serum albumen (BSA) in PBS. Sections were first incubated with the indicated primary antibodies in blocking solution without 0.2% Triton X-100 at 4°C for 16 h and then with the appropriate Alexa488-, Cy3-, or Cy5-conjugated secondary antibody. Immunofluorescence was subsequently analyzed using Olympus FV1000 and Zeiss LSM710 confocal microscopes.

Isolation and detection of extracellular proteins in growth media and CSF

Growth medium or CSF from the lateral ventricle of E14.5 mice was centrifuged twice at $500 \times g$ for 10 min and then twice at $2,000 \times g$ for 15 min to obtain supernatant (S3) fractions. The S3 fractions were then mixed with an equal volume of 3 M trichloroacetic acid (TCA) solution to precipitate macromolecules. The TCA precipitates were washed twice with 100% acetone, air-dried pellets, and dissolved in 2 \times -sodium dodecyl sulfate (SDS) sample buffer for SDS-PAGE (polyacrylamide gel electrophoresis) analysis.

477

478 ***Drosophila* lines and whole-mount immunostaining**

479 *Ptc-Gal4*, *UAS-DsRed*, *UAS-Sdc*, *UAS-Dlp*, and *sdc*²³ flies were obtained from the
 480 Bloomington stock center. The *UAS-Vax1-EGFP* fly was generated by injection of pUAS-
 481 *Vax1-EGFP*, constructed by cloning mouse *Vax1* cDNA into the pUAST-EGFP vector.
 482 Third instar larvae of *Ptc-Gal4>UAS-Vax1-EGFP;UAS-DsRed*;+ were obtained from a
 483 cross of the *Ptc-Gal4>UAS-DsRed;TM6B* fly with a *UAS-Vax1-EGFP* fly.

484 After fixing larval wing imaginal discs with 4% PFA/PBS for 30 min, the *Ptc-Gal4*-
 485 induced green fluorescence signals from EGFP and *Vax1-EGFP* proteins were compared
 486 with red fluorescence signals from *DsRed* proteins by confocal microscopy (Olympus
 487 FV1000). Prior to fixing, extracellular *Vax1* protein was detected by sequentially incubating
 488 *Drosophila* wing imaginal discs with α -*Vax1* (1:10; for 10 min on ice) and Cy5-conjugated
 489 donkey anti-rabbit IgG (1 h), and then analyzed by confocal microscopy.

490

491 ***Co-immunoprecipitation***

492 HEK293T cells and E14.5 mouse optic nerves were lysed in a buffer consisting of 10 mM
 493 Tris-HCl (pH 7.4), 200 mM NaCl, 1% Triton X-100, and 1% NP-40. Cell lysates were
 494 centrifuged at 12,000 \times g for 10 min at 4°C. The supernatants were collected and
 495 incubated with the indicated antibodies at 4°C for 16 h; then, Protein A-agarose beads
 496 were added and incubation was continued at 4°C for 1 h. After washing the immune
 497 complexes five times with lysis buffer, proteins were eluted with 2 \times SDS sample buffer.
 498 Samples were then analyzed by SDS-PAGE and Western blotting.

499

500 ***GST-affinity purification of Vax1-interacting proteins***

501 HEK293T cells transfected with pEBG or pEBG-*Vax1* were lysed with a buffer consisting
 502 of 10 mM Tris-HCl (pH 7.4), 200 mM NaCl, and 1% NP-40. Cell lysates were centrifuged
 503 at 12,000 \times g for 10 min at 4°C. The supernatants were collected and incubated with
 504 glutathione Sepharose 4B resin (GE Healthcare) at 4°C for 1 h. After washing five times
 505 with lysis buffer, proteins were eluted with 2 \times SDS sample buffer, and samples were
 506 analyzed by SDS-PAGE on 10% gels. Gels were stained using Silver Stain Kit for Mass
 507 Spectrometry (Pierce) to isolate bands for MALDI-TOF mass spectrometry analysis at the
 508 Korea Basic Science Institute (KBSI), Daejeon, South Korea.

509

Click chemistry for labeling newly synthesized proteins

Explant culture media were replaced with methionine-free media 30 min prior to the addition of 50 μ M L-azidohomoalanine (AHA; Invitrogen). After 6 h, retinal explants were washed twice with PBS containing 1% fetal bovine serum (FBS), and then 30 μ M DIBO-Alexa Fluor 488 (Invitrogen) in PBS containing 1% FBS was added. The explants were then incubated at room temperature in the dark for 1 h. After washing four times in PBS containing 1% FBS, retinal explants were fixed with 4% PFA in PBS for 15 min at room temperature for subsequent detection of the fluorescence of proteins incorporating AHA-Alexa Fluor 488.

Acknowledgements

We thank Dr. Greg Lemke, Dr. Peter Gruss, and Dr. Eok-Soo Oh for providing *Vax1-ko* mice, *Vax1^{lacZ}* knock-in mice and GFP-Sdc2 constructs, respectively. We also thank to Dr. Jong Soon Choi for the support with MALDI-TOF mass spectrometry analysis. This work was supported by grants from the Global Research Laboratory Program (NRF-2009-00424; JWK), Brain Research Program (NRF-2013-056566; JWK), Basic Science Research Program (NRF-2014R1A2A2A01003069; JWK), and Stem Cell Research Program (NRF-2006-2004289; KHK) funded by the Korean Ministry of Science, ICT, and Future Planning (MSIP). This study was performed in strict accordance with the recommendations in the Guide for the Care and Use of Laboratory Animals of the Korean Ministry of Agriculture, Food and Rural Affairs. All of the animals were handled according to approved institutional animal care and use committee (IACUC) protocols (#13-130) of Korea Advanced Institute of Science and Technology.

References

Barbieri AM, Lupo G, Bulfone A, Andreazzoli M, Mariani M, Fougerousse F, Consalez GG, Borsani G, Beckmann JS, Barsacchi G, Ballabio A, Banfi S (1999) A homeobox gene, *vax2*, controls the patterning of the eye dorsoventral axis. *Proc Natl Acad Sci U S A* **96**: 10729-10734

543 Bertuzzi S, Hindges R, Mui SH, O'Leary DD, Lemke G (1999) The homeodomain protein
544 *vax1* is required for axon guidance and major tract formation in the developing forebrain.
545 *Genes Dev* **13**: 3092-3105
546

547 Beurdeley M, Spatazza J, Lee HH, Sugiyama S, Bernard C, Di Nardo AA, Hensch TK,
548 Prochiantz A (2012) Otx2 binding to perineuronal nets persistently regulates plasticity in
549 the mature visual cortex. *J Neurosci* **32**: 9429-9437
550

551 Bishop JR, Schuksz M, Esko JD (2007) Heparan sulphate proteoglycans fine-tune
552 mammalian physiology. *Nature* **446**: 1030-1037
553

554 Brunet I, Weinl C, Piper M, Trembleau A, Volovitch M, Harris W, Prochiantz A, Holt C
555 (2005) The transcription factor Engrailed-2 guides retinal axons. *Nature* **438**: 94-98
556

557 Bürglin TR (2011) Homeodomain subtypes and functional diversity. *A handbook of*
558 *transcription factors*: 95-122
559

560 Charron F, Stein E, Jeong J, McMahon AP, Tessier-Lavigne M (2003) The morphogen
561 sonic hedgehog is an axonal chemoattractant that collaborates with netrin-1 in midline
562 axon guidance. *Cell* **113**: 11-23
563

564 Chung KY, Leung KM, Lin L, Chan SO (2001) Heparan sulfate proteoglycan expression in
565 the optic chiasm of mouse embryos. *J Comp Neurol* **436**: 236-247
566

567 Deiner MS, Sretavan DW (1999) Altered midline axon pathways and ectopic neurons in
568 the developing hypothalamus of netrin-1- and DCC-deficient mice. *J Neurosci* **19**: 9900-
569 9912
570

571 Dieterich DC, Lee JJ, Link AJ, Graumann J, Tirrell DA, Schuman EM (2007) Labeling,
572 detection and identification of newly synthesized proteomes with bioorthogonal non-
573 canonical amino-acid tagging. *Nat Protoc* **2**: 532-540
574

575 Erskine L, Herrera E (2007) The retinal ganglion cell axon's journey: insights into
576 molecular mechanisms of axon guidance. *Dev Biol* **308**: 1-14
577

578 Erskine L, Reijntjes S, Pratt T, Denti L, Schwarz Q, Vieira JM, Alakakone B, Shewan D,
579 Ruhrberg C (2011) VEGF signaling through neuropilin 1 guides commissural axon
580 crossing at the optic chiasm. *Neuron* **70**: 951-965
581

582 Erskine L, Williams SE, Brose K, Kidd T, Rachel RA, Goodman CS, Tessier-Lavigne M,
583 Mason CA (2000) Retinal ganglion cell axon guidance in the mouse optic chiasm:
584 expression and function of *robo*s and *slits*. *J Neurosci* **20**: 4975-4982
585

586 Hallonet M, Hollemann T, Pieler T, Gruss P (1999) *Vax1*, a novel homeobox-containing
587 gene, directs development of the basal forebrain and visual system. *Genes Dev* **13**: 3106-
588 3114
589

590 Hallonet M, Hollemann T, Wehr R, Jenkins NA, Copeland NG, Pieler T, Gruss P (1998)
591 *Vax1* is a novel homeobox-containing gene expressed in the developing anterior ventral
592 forebrain. *Development* **125**: 2599-2610

- Hussain SA, Piper M, Fukuhara N, Strohlic L, Cho G, Howitt JA, Ahmed Y, Powell AK, Turnbull JE, Holt CE, Hohenester E (2006) A molecular mechanism for the heparan sulfate dependence of slit-robo signaling. *J Biol Chem* **281**: 39693-39698
- Inatani M, Irie F, Plump AS, Tessier-Lavigne M, Yamaguchi Y (2003) Mammalian brain morphogenesis and midline axon guidance require heparan sulfate. *Science* **302**: 1044-1046
- Johnson KG, Ghose A, Epstein E, Lincecum J, O'Connor MB, Van Vactor D (2004) Axonal heparan sulfate proteoglycans regulate the distribution and efficiency of the repellent slit during midline axon guidance. *Curr Biol* **14**: 499-504
- Joliot A, Maizel A, Rosenberg D, Trembleau A, Dupas S, Volovitch M, Prochiantz A (1998) Identification of a signal sequence necessary for the unconventional secretion of Engrailed homeoprotein. *Curr Biol* **8**: 856-863
- Joliot A, Prochiantz A (2004) Transduction peptides: from technology to physiology. *Nat Cell Biol* **6**: 189-196
- Kantor DB, Chivatakarn O, Peer KL, Oster SF, Inatani M, Hansen MJ, Flanagan JG, Yamaguchi Y, Sretavan DW, Giger RJ, Kolodkin AL (2004) Semaphorin 5A is a bifunctional axon guidance cue regulated by heparan and chondroitin sulfate proteoglycans. *Neuron* **44**: 961-975
- Kim JW, Lemke G (2006) Hedgehog-regulated localization of Vax2 controls eye development. *Genes Dev* **20**: 2833-2847
- Kuwajima T, Yoshida Y, Takegahara N, Petros TJ, Kumanogoh A, Jessell TM, Sakurai T, Mason C (2012) Optic chiasm presentation of Semaphorin6D in the context of Plexin-A1 and Nr-CAM promotes retinal axon midline crossing. *Neuron* **74**: 676-690
- Lee JS, Chien CB (2004) When sugars guide axons: insights from heparan sulphate proteoglycan mutants. *Nat Rev Genet* **5**: 923-935
- Lemke G, Reber M (2005) Retinotectal mapping: new insights from molecular genetics. *Annu Rev Cell Dev Biol* **21**: 551-580
- Maizel A, Tassetto M, Filhol O, Cochet C, Prochiantz A, Joliot A (2002) Engrailed homeoprotein secretion is a regulated process. *Development* **129**: 3545-3553
- Matsumoto Y, Irie F, Inatani M, Tessier-Lavigne M, Yamaguchi Y (2007) Netrin-1/DCC signaling in commissural axon guidance requires cell-autonomous expression of heparan sulfate. *J Neurosci* **27**: 4342-4350
- Miyata S, Komatsu Y, Yoshimura Y, Taya C, Kitagawa H (2012) Persistent cortical plasticity by upregulation of chondroitin 6-sulfation. *Nat Neurosci* **15**: 414-422, S411-412
- Mui SH, Kim JW, Lemke G, Bertuzzi S (2005) Vax genes ventralize the embryonic eye. *Genes Dev* **19**: 1249-1259

- Nakagawa S, Brennan C, Johnson KG, Shewan D, Harris WA, Holt CE (2000) Ephrin-B regulates the Ipsilateral routing of retinal axons at the optic chiasm. *Neuron* **25**: 599-610
- Ogata-Iwao M, Inatani M, Iwao K, Takihara Y, Nakaishi-Fukuchi Y, Irie F, Sato S, Furukawa T, Yamaguchi Y, Tanihara H (2011) Heparan sulfate regulates intraretinal axon pathfinding by retinal ganglion cells. *Invest Ophthalmol Vis Sci* **52**: 6671-6679
- Petros TJ, Rebsam A, Mason CA (2008) Retinal axon growth at the optic chiasm: to cross or not to cross. *Annu Rev Neurosci* **31**: 295-315
- Piper M, Anderson R, Dwivedy A, Weinl C, van Horck F, Leung KM, Cogill E, Holt C (2006) Signaling mechanisms underlying Slit2-induced collapse of *Xenopus* retinal growth cones. *Neuron* **49**: 215-228
- Plump AS, Erskine L, Sabatier C, Brose K, Epstein CJ, Goodman CS, Mason CA, Tessier-Lavigne M (2002) Slit1 and Slit2 cooperate to prevent premature midline crossing of retinal axons in the mouse visual system. *Neuron* **33**: 219-232
- Pratt T, Conway CD, Tian NM, Price DJ, Mason JO (2006) Heparan sulphation patterns generated by specific heparan sulfotransferase enzymes direct distinct aspects of retinal axon guidance at the optic chiasm. *J Neurosci* **26**: 6911-6923
- Sanchez-Camacho C, Bovolenta P (2008) Autonomous and non-autonomous Shh signalling mediate the in vivo growth and guidance of mouse retinal ganglion cell axons. *Development* **135**: 3531-3541
- Sato M, Lopez-Mascaraque L, Heffner CD, O'Leary DD (1994) Action of a diffusible target-derived chemoattractant on cortical axon branch induction and directed growth. *Neuron* **13**: 791-803
- Slavotinek AM, Chao R, Vacik T, Yahyavi M, Abouzeid H, Bardakjian T, Schneider A, Shaw G, Sherr EH, Lemke G, Youssef M, Schorderet DF (2012) VAX1 mutation associated with microphthalmia, corpus callosum agenesis, and orofacial clefting: the first description of a VAX1 phenotype in humans. *Hum Mutat* **33**: 364-368
- Soker S, Fidler IJ, Neufeld G, Klagsbrun M (1996) Characterization of novel vascular endothelial growth factor (VEGF) receptors on tumor cells that bind VEGF165 via its exon 7-encoded domain. *J Biol Chem* **271**: 5761-5767
- Spatazza J, Di Lullo E, Joliot A, Dupont E, Moya KL, Prochiantz A (2013) Homeoprotein signaling in development, health, and disease: a shaking of dogmas offers challenges and promises from bench to bed. *Pharmacol Rev* **65**: 90-104
- Spring J, Paine-Saunders SE, Hynes RO, Bernfield M (1994) Drosophila syndecan: conservation of a cell-surface heparan sulfate proteoglycan. *Proc Natl Acad Sci U S A* **91**: 3334-3338

691 Stein E, Tessier-Lavigne M (2001) Hierarchical organization of guidance receptors:
692 silencing of netrin attraction by slit through a Robo/DCC receptor complex. *Science* **291**:
693 1928-1938
694
695 Stettler O, Joshi RL, Wizenmann A, Reingruber J, Holcman D, Bouillot C, Castagner F,
696 Prochiantz A, Moya KL (2012) Engrailed homeoprotein recruits the adenosine A1 receptor
697 to potentiate ephrin A5 function in retinal growth cones. *Development* **139**: 215-224
698
699 Sugiyama S, Di Nardo AA, Aizawa S, Matsuo I, Volovitch M, Prochiantz A, Hensch TK
700 (2008) Experience-dependent transfer of Otx2 homeoprotein into the visual cortex
701 activates postnatal plasticity. *Cell* **134**: 508-520
702
703 Vacik T, Stubbs JL, Lemke G (2011) A novel mechanism for the transcriptional regulation
704 of Wnt signaling in development. *Genes Dev* **25**: 1783-1795
705
706 Williams SE, Grumet M, Colman DR, Henkemeyer M, Mason CA, Sakurai T (2006) A role
707 for Nr-CAM in the patterning of binocular visual pathways. *Neuron* **50**: 535-547
708
709 Williams SE, Mann F, Erskine L, Sakurai T, Wei S, Rossi DJ, Gale NW, Holt CE, Mason
710 CA, Henkemeyer M (2003) Ephrin-B2 and EphB1 mediate retinal axon divergence at the
711 optic chiasm. *Neuron* **39**: 919-935
712
713 Wright KM, Lyon KA, Leung H, Leahy DJ, Ma L, Ginty DD (2012) Dystroglycan organizes
714 axon guidance cue localization and axonal pathfinding. *Neuron* **76**: 931-944
715
716 Yoon BC, Jung H, Dwivedy A, O'Hare CM, Zivraj KH, Holt CE (2012) Local translation of
717 extranuclear lamin B promotes axon maintenance. *Cell* **148**: 752-764
718
719
720

Figure legends

Figure 1. Vax1 regulates RGC axonal growth in a non-cell autonomous manner. (A) Cells expressing Vax1 (green) in brain sections (coronal; 16 μm) from E14.5 *Vax1*^{+/+} (top) and *Vax1*^{-/-} (bottom) embryos were detected by co-immunostaining for the NPC marker Sox2 (red) and post-mitotic neuronal marker tubulin- β III (blue), detected with the Tuj1 antibody. The right-most three columns are magnified images of dotted boxes in the left column image. The results indicate that Vax1 is expressed in a subpopulation of Sox2-positive NPCs (arrowheads), but is not detectable in Tuj1-positive neurons. (B) Vax1-expressing cells in the vHT were also compared with RC2-positive radial glia. Arrowheads indicate RC2-positive radial glial cells expressing Vax1. Scale bars: 50 μm . (C) The vHT and dorsal neural retina (NR) were isolated from WT (*Vax1*^{+/+}) and *Vax1*-knockout (*Vax1*^{-/-}) E13.5 mouse embryos and co-cultured in a combinatorial manner for 48 h. The explants were fixed and immunostained with an anti-NF160 antibody (α -NF160; red); nuclei were counterstained with DAPI (blue). Dotted boxes indicate the area magnified in each inset. Red dotted lines link centers of retinal explants and vHT explants. Scale bars: 500 μm . (D) The angular distribution of RGC axons in images was measured by counting pixels containing immunostaining for the axon marker NF160 (axon counts), as described in Materials and methods, and presented graphically. +, forward direction angle segment; 0, neutral direction angle segments; -, reverse direction angle segment. The values in the bar are averages, error bars denote standard deviations (SDs), and numbers under y-axis labels are the numbers (n) of explants analyzed from three independent experiments. *P*-values determined by analysis of variance (ANOVA) are between 0.01 and 0.005.

Figure 2. Vax1 homeodomain protein is a secreted protein. (A) COS7 cells overexpressing Myc-tagged mouse Vax1, Vax1(R152S), or Vax2 were co-cultured with E13.5 mouse retinal explants (NR) for 48 h. The explants were then stained with a rabbit anti-Myc antibody (green) and a mouse anti-NF160 antibody (red). Nuclei of explant cells were counterstained with DAPI (blue). Dotted red lines indicate the connections between the centers of two explants. Scale bars: 500 μm (left column) and 100 μm (magnified immunostained images in two right-hand columns). (B) The angular distribution of RGC axons was measured as described in Figure 1D. The values in the bar are averages, and error bars denote SDs. Numbers under y-axis labels are the numbers of explants analyzed

from three independent experiments. *P*-values are between 0.01 and 0.005 (ANOVA). (C) Growth medium from COS7 cells overexpressing Myc-Vax1, Myc-Vax1(R152S), or Myc-Vax2 was collected, and the presence of Vax protein in the growth medium (GM) was detected by Western blotting (WB) with an anti-Myc antibody. The relative amounts of secreted protein were also measured by analyzing the levels of proteins in COS7 cell lysates (CL; 5% of total). (D) vHTs isolated from WT and *Vax1*-deficient E13.5 mouse embryos were cultured for 24 h, after which GM was collected for detection of secreted Vax1 protein by Western blotting. CL, cell lysates of vHT explants (5% of total). (E) Cerebrospinal fluid (CSF) from E14.5 mouse embryos was collected, a supernatant fraction (S3) was separated from cell debris (P2) by step-wise centrifugation, and the presence of Vax1 protein was examined by Western blotting. The presence of β -tubulin, a cytoplasmic protein, was also examined in GM and CSF fractions to check for possible non-specific release of intracellular proteins from dead cells. CL, E14.5 vHT cell lysates (2% of total).

Figure 3. Vax1 protein is a retinal axon growth factor. (A) E13.5 mouse retinal explants were cultured for 24 h and then treated with 6X-His-FITC peptide (100 ng/ml) or recombinant Vax1-His-FITC protein (500 ng/ml) for an additional 24 h. Images of RGC axons were taken every 15 min for 16 h before immunostaining with anti-Vax1 and anti-His antibodies (Video supplements 1 and 2; Figure 3 – figure supplement 1). The accumulation of Vax1-His in growing RGC axons was also visualized by detecting FITC fluorescence signals (inset images). Red arrowheads indicate the area magnified in each inset. (B) The changes in RGC axonal length during the recording were plotted after adjusting the initial length to 100%. (C) Retinal explants treated with 6X-His (25 ng/ml), Vax1 (100 ng/ml), or Vax1(R152S) (100 ng/ml) for 24 h were stained with rabbit anti-Vax1 (green) and mouse anti-NF160 (red) antibodies to visualize Vax1 protein in RGC axons. Arrowheads indicate the area magnified in each inset. Scale bars: 500 μ m. (D) Relative numbers of axon bundles projecting from retinal explants were indirectly measured by counting the pixels containing NF160 immunofluorescence in RGC axons between 20 and 40 μ m from the rim of the explants (total axon bundle). The relative thickness of individual axon bundles was also measured by comparing total pixel counts of NF160 in the 20–40- μ m area (individual axon bundle). The values in the graph are averages expressed relative to those of 6X-His peptide-treated samples, presented as 1; error bars denote SDs

(** $p < 0.001$; ANOVA). The scores on top of graph columns are the numbers of axons (individual axon bundle) and the numbers of explants (total axon bundle) analyzed, respectively. Results were obtained from three independent experiments. Numbers of explants analyzed: for 6X-His, $n=10$; Vax1-His, $n=11$; Vax1(R152S)-His, $n=6$. (already shown in total axon bundle)

Figure 4. Mouse RGC axons import Vax1 protein. (A) Vax1 mRNA expression in E14.5 WT ($Vax1^{+/+}$) mouse retinas was examined by *in situ* RNA hybridization using a [33 P]-CTP-labeled antisense Vax1 probe, as described elsewhere (Mui et al, 2005). Vax1 transcripts were detected in the OS and OD, but not in the neural retina (NR). This *in situ* hybridization signal was absent in $Vax1^{lacZ/lacZ}$ homozygous knock-in mouse eyes (bottom). (B) The distribution of Vax1 protein in the NR (i and iii) and OS (ii and iv) of E14.5 $Vax1^{lacZ/+}$ and $Vax1^{lacZ/lacZ}$ embryos was compared with that of β -gal expressed from the *lacZ* gene at the Vax1 locus by co-staining with rabbit anti-Vax1 (green) and mouse anti- β -gal (red) antibodies. Vax1 protein detected in $Vax1^{lacZ/+}$ mouse retinal cells, where β -gal signals were absent, are presumed to originate from external sources that co-express Vax1 and β -gal. Red dots in (iii) are non-specific background β -gal immunostaining. (C) Distribution of Vax1 in RGC axons and cell bodies was examined by co-immunostaining for Vax1 (green) and the RGC axonal marker NF160 (red). Nuclei were counterstained with DAPI (blue). Arrowheads in (ii) indicate Vax1 protein that co-localizes with NF160, whereas arrows point to Vax1 in APC nuclei. Vax1 immunostaining signals were completely absent in the OS and NR of $Vax1^{lacZ/lacZ}$ mice, whereas NF160 immunostaining was still detectable in defasciculated RGC axons (iii and iv). (D) Sections of E18.5 WT and $Vax1^{lacZ/lacZ}$ mouse retinas (top) and optic nerves (ON; bottom) were immunostained with rabbit anti-Vax1 antibody and gold (25 nm)-labeled anti-rabbit IgG. Subcellular localization of Vax1 proteins was then examined by electron microscopy. Arrowheads in RGC images point to Vax1 proteins in the intracellular vesicle, whereas arrows in the images indicate Vax1 proteins bound to the extracellular surface of the RGC plasma membrane (top). Arrowheads in APC images indicate Vax1 proteins in trafficking vesicles, whereas arrows mark Vax1 proteins associated with chromatin in the nucleus (bottom). Scale bars in (A) to (C): 200 μ m (left column) and 20 μ m (right two columns). Scale bars in (D): 0.5 μ m (left columns) and 0.2 μ m (right two columns).

Figure 5. Secreted Vax1 protein is necessary for RGC axon growth. (A) vHTs and retinas isolated from E13.5 mouse embryos were co-cultured for 48 h in the presence of pre-immune rabbit IgG (rb-IgG; 1 μ g/ml), anti-Vax1 (α -Vax1; 1 μ g/ml), or anti-Vax2 (α -Vax2; 1 μ g/ml) antibodies. Vax1 localization in RGC axons was then determined by staining explants with rabbit α -Vax1 (green) and mouse α -NF160 (red). Arrowheads indicate the area magnified in each inset. Scale bars: 500 μ m. (B) The distribution of RGC axons in each angle segment was determined as described in Materials and methods. The values in the bar are averages, and error bars denote SDs. *P*-values are between 0.01 and 0.005 (ANOVA). (C) Total image pixel counts of NF160 immunofluorescence in a 20–40- μ m area were compared to obtain the relative number of axons projected from each explant. Scores under *y*-axis labels of (B) and (C) are the numbers of explants analyzed in three independent experiments (***p*<0.001; ANOVA). (D) Slabs of mouse heads including eyes, forebrain, and midbrain structures were prepared from E13.5 WT mouse embryos. The third brain ventricles of mouse-head slabs were then implanted with collagen gels containing rb-IgG (1 μ g/ml) or α -Vax1 (1 μ g/ml) and subsequently incubated at 37°C in a CO₂ incubator for 12 h (top row; see Materials and methods for details). The slabs were then fixed and frozen to obtain horizontal sections (18 μ m thick). The slides containing optic nerves (ON) were then further stained with rabbit α -Vax1 (green) and mouse α -NF160 (red) and analyzed using an Olympus FV1000 confocal microscope. Images in the bottom row are magnifications of dotted boxes in the top row. Scale bars: 200 μ m. Relative fluorescence intensities of Vax1- and/or NF160-positive immunostaining intensities in the midline area (dotted box) were measured using Image-J software and presented graphically. White column, rb-IgG; black column, α -Vax1. The values are relative intensities compared with rb-IgG-treated samples; error bars denote SD and values on top of graph columns are number of slabs analyzed (**p*<0.01; Student *t*-test). A, anterior; P, posterior; M, medial; L, lateral; *, optic chiasm; V3, third ventricle.

Figure 6. Regulation of intercellular Vax1 transfer by HSPGs in *Drosophila* wing imaginal discs. Vax1-EGFP (green) and DsRed (red) were co-expressed under the control of *Ptc-Gal4* in the A/P boundary cells of *Drosophila* wing imaginal discs in *wt* (top row) and *Sdc* mutant (*Sdc*²³; second row) flies. The number of cells positive for Vax1-EGFP but negative for DsRed at the posterior part of the wing disc was increased in *Sdc*²³ flies. In contrast, the number of Vax1-EGFP-positive cells in the posterior wing disc was significantly

decreased in fly embryos that co-expressed Sdc (third row) or Dlp (bottom row) together with Vax1-EGFP and DsRed. Diagrams in the right column show the distribution of Vax1-EGFP-positive cells (green) and DsRed (red) in the corresponding fly wing discs. Scale bars: 100 μ m.

Figure 7. Vax1 binding to HSPGs is necessary for RGC axonal growth. (A) Interaction between Vax1 and Sdc2 in the E14.5 mouse OS was investigated by immunoprecipitation with a rabbit anti-Vax1 (top) or goat anti-Sdc2 (bottom) antibody and subsequent Western blotting with reciprocal antibodies. The specificity of anti-Vax1 and anti-Sdc2 antibodies was confirmed by immunoprecipitation with pre-immune rabbit IgG (rb-IgG) and goat IgG (gt-IgG), respectively. (B) Immunoprecipitation of Vax1 in the E14.5 mouse OS was also performed in the presence or absence of heparin (1 mg/ml) to determine whether Vax1 protein bound to HS sugar groups of Sdc2, Sdc3, and/or Glp1 HSPGs expressed in RGC axons. (C) Vax1-His protein (final concentration, 2 μ g/ml) was incubated at 4°C for 1 h with Sepharose 4B resin (Sigma) coated with HS or CS. The resins were washed three times with PBS, and Vax1 protein bound to the resins was eluted in SDS sample buffer for subsequent SDS-PAGE on 10% gels and Western blotting with α -Vax1. Relative intensities of Vax1 bands in Western blot images were analyzed using Image-J software. (D) Retinal explants were treated with heparinase I (2.5 U/ml) or ChnaseABC (2.5 U/ml) for 3 h and then incubated with 6X-His peptide (25 ng/ml) or Vax1-His recombinant protein (100 ng/ml) for an additional 24 h. The presence of Vax1-His in RGC axons was then examined by co-immunostaining with rabbit anti-Vax1 (green), mouse anti-NF160 (red), and goat anti-Sdc3 (blue) antibodies. Dotted boxes indicate the area magnified at right. Scale bars: 500 μ m. (E) The graph shows relative distances that RGC axons grew during the 24-h incubation period. The values in the graph are averages of fold ratios compared with those of 6X-His-treated samples, error bars denote SDs, and the scores on top of graph columns are the numbers of axons analyzed (* p <0.01, ** p <0.001; ANOVA). Results were obtained from three independent experiments. Numbers of explants analyzed: 6X-His, n =6; Vax1, n =7; heparinase, n =5; chondroitinase, n =5; Vax1+heparinase I, n =6; Vax1+ChnaseABC, n =6.

Figure 8. Imported Vax1 induces RGC axonal growth by stimulating local protein synthesis. (A) GST and GST-Vax1 protein complexes were affinity purified from

cytoplasmic fractions of HEK293T cells overexpressing GST and GST-Vax1, respectively (see Materials and methods for details). Complexes were then analyzed by SDS-PAGE on 10% gels and subsequent silver staining to detect proteins specifically enriched in GST-Vax1 complexes. The identities of protein bands, shown to the right of the gel photograph, were determined by MALDI-TOF mass spectrometry. Vax1-FL, full-length Vax1; Vax1-N*, Vax1 N-terminal fragment. (B) E13.5 mouse retinal explants were cultured for 24 h before changing to medium containing Vax1-His (100 ng/ml) or Vax1(WF/SR)-His (100 ng/ml) for an additional 16 h-incubation. The explants were further incubated for 6 h after addition of the bioorthogonal, noncanonical amino acid AHA (L-azidohomoalanine). Newly synthesized proteins incorporating these noncanonical amino acids were labeled with Alexa Fluor 488-alkyne by click chemistry (Dieterich et al, 2007), and the rates of protein synthesis in RGC axons (middle row) and explant cell body (bottom) were assessed by measuring the fluorescence intensities of AHA-Alexa Fluor 488-labeled proteins (see Materials and methods for details). Scale bars: 500 μ m (top) and 100 μ m (bottom). (C) The influence of nuclear events in Vax1-induced RGC axon growth was excluded by isolating axons from the cell body before treatment with Vax1 protein (100 ng/ml) for 6 h. Arrowheads indicate the area magnified in each inset. Scale bars: 500 μ m. (D) Relative AHA-Alexa488 fluorescence intensities in cell body-free axons were measured using Image-J software and are shown graphically. Error bars denote SD. (E) Relative distances that RGC axons grew during this 6-h incubation period are presented graphically. The values in the graph are averages of fold ratios compared with those of untreated samples. Scores on top of graph columns in (D) and (E) are numbers of axons analyzed (**p<0.001; ANOVA). Results were obtained from two independent experiments. Numbers of explants analyzed: untreated, n=4; Vax1, n=5; Vax1(WF/SR), n=4.

Figure 9. RGC axons regrow in Vax1-implanted, Vax1-deficient mouse brains. (A) The third ventricles of E13.5 Vax1-deficient (*Vax1^{lacZ/lacZ}*) mouse-head slabs were implanted with collagen gels mixed with 6X-His peptide (4.78 μ g/ml; 5.69 nmol), Vax1-His (200 μ g/ml; 5.69 nmol), or Vax1(WF/SR)-His (200 μ g/ml; 5.69 nmol) and incubated for 12 h (see diagram in Figure 5D and Materials and methods for details). Vax1-deficient mouse-head slabs were also implanted with collagen gels mixed with Robo1-Fc fragment (1 μ g/ml; 12.35 pmol; R&D Systems) in the presence of 6X-His peptide (4.78 μ g/ml; 5.69 nmol) or Vax1-His (200 μ g/ml; 5.69 nmol) and incubated for 12 h. The fluorescence images of

horizontal sections of head slabs were obtained using an Olympus FV1000 confocal microscopy equipped with a transmitted light detector (top row). The same embryonic sections were further stained with rabbit anti-Vax1 (green) and mouse anti-NF160 (red) antibodies (bottom row). (B) Fluorescence intensities of NF160 immunostains in the boxed areas in (A) were measured using Image-J software and are presented graphically. The values are intensities expressed relative to rb-IgG-treated samples, and error bars denote SDs (** $p < 0.001$; ANOVA). Numbers on top of graph columns are head-slab preparations.

Figure 10. Model depicting Vax1 function as a secreted retinal axon growth factor. Vax1 is expressed in radial glia and NPCs of the vHT as well as OS APCs (A) and secreted to the extracellular space (B). RGC axons that grow in the OS capture APC-secreted Vax1 by HSPGs, resulting in an increase in Vax1 concentration at RGC axons for subsequent penetration and local activation of translation in the axon (B). The imported Vax1 in RGC axoplasm not only promotes axonal growth toward the vHT, but it also enhances fasciculation of RGC axons. This axon growth-stimulatory activity of Vax1 supports sustained RGC axon growth to the vHT midline after the axons were avoided from progressing to dorsal diencephalon, which expresses high concentration of Slit repulsive axon guidance cue (C, top). Therefore, RGC axons stop at the lateral wall of *Vax1-ko* mouse diencephalon and fail to access the midline (C, bottom). At the vHT midline, RGC axon guidance cues, including VEGF164, NrCAM and ephrinB2, determine the directionalities of RGC axon growth cones by acting their specific receptors (D). Vax1 does not likely determine the directionalities of RGC axon growth cone at the midline but does promote the growth of the RGC axon shaft as well as the growth cone regardless of their original positions in the retina.

Figure supplements

Figure 1 – figure supplement 1. To determine whether defective projection of RGC axons to the vHT midline of *Vax1*-ko mice resulted from defective expression of RGC axon growth factors, such as VEGF164 or NrCAM (Erskine et al, 2011; Williams et al, 2006), in the vHT, we compared expression of these cues between WT (*Vax1*^{+/+}) and *Vax1*-knockout (*Vax1*^{-/-}) mouse embryos. Expression of *Vegfa* mRNA (A) and NrCAM protein in E14.5 *Vax1*^{+/+} and *Vax1*^{-/-} mouse embryonic sections (coronal; 16 µm) was examined by *in situ* RNA hybridization (ISH; A) and immunofluorescence staining (IF; B), respectively. The vHT of the *Vax1*^{-/-} mouse brain retained, but expanded, expression of both *Vegfa* and NrCAM. Scale bars: 100 µm.

Figure 2 – figure supplement 1. Relative transcriptional activities of *Vax1* mutants used in this study. HEK293T cells (10⁵) were transfected with pcDNA6-V5 expression vectors (1 µg) for *Vax1*, *Vax1*(R152S), or *Vax1*(WF/SR) together with pGL3-Tcf711-luciferase (0.2 µg) (Vacik et al, 2011) and pCMV-β-gal (0.2 µg) plasmids. Luciferase activity in the transfected cells was measured 24 h post-transfection. The values were then normalized to β-galactosidase activity in the same cells to obtain the relative luciferase activity of the cells. The values are averages obtained from three independent experiments, and error bars denote SD (***p*<0.001; ANOVA).

Figure 2 – figure supplement 2. Interference of *Vax1* intercellular transfer by sequestering extracellular *Vax1*. E13.5 retinal explants were co-incubated with Myc-*Vax1* transfected COS7 cell aggregates for 24 h in the presence rb-IgG (1 µg/ml; top) or anti-*Vax1* antibody (α-*Vax1*; 1 µg/ml; bottom). The explants were then fixed for immunostaining with mouse anti-NF160 antibody (red) and rabbit anti-Myc antibody (green). Immunostaining images of dotted boxed area in left column are shown in right column. Arrows indicate *Vax1*-Myc proteins internalized to RGC axons. Scale bars: left, 500 µm; right, 100 µm.

Figure 3 – figure supplement 1. Penetration of exogenous *Vax1* protein into RGC axons. Retinal explants isolated from E13.5 mouse embryos were cultured for 24 h before recording phase contrast and fluorescence images every 15 min on a Zeiss Axio Observer

Z1 inverted microscope. After 180 min of recording, 6X-His-FITC peptide (100 ng/ml) or Vax1-His-FITC protein (500 ng/ml) was added to the growth medium. The images were then combined into movie clips, provided in Video supplement 1 and 2. After recording for 16 h, the explants were washed with PBS, and Vax1 protein present at the surface of axons was detected by incubating with rabbit α -Vax1 (green) in growth medium for 20 min. The explants were then washed three times with PBS and fixed in 4% PFS/PBS for 1 h prior to the detection of 6X-His peptide or Vax1-His protein inside and on the surface of axons using mouse anti-His antibody (red). The explants were then further incubated with Alexa 488-labeled α -rabbit IgG and Cy3-labeled α -mouse IgG, and the distribution of Vax1 on the surface and within the intracellular space of RGC axons was analyzed by confocal microscopy. Phase contrast images in the left column show representative snapshot images from Video supplement 1 and 2. Immunostained images in the right columns correspond to dotted boxes in the phase contrast images in the left column. Arrows indicate Vax1-His proteins internalized to RGC axons. Scale bars: 100 μ m.

Figure 3 – figure supplement 2. Region non-selective stimulation of retinal axonal growth by recombinant Vax1. Dark field images of retinal quadrant explants were taken before (0 h) and after (24 h) treating them with 6X-His peptide (25 ng/ml; white column) or Vax1-His protein (100 ng/ml; black column). The changes in axonal length during the 24-h incubation period were shown in a graph. The values in the graph are averages and error bars denote SD. The scores in the graph columns are the numbers of axons analyzed. Numbers of explants analyzed are shown on top of the columns. *P*-values were determined by Student *t*-test (**, *p*<0.001). Results were obtained from two independent experiments.

Figure 3 – figure supplement 3. Recombinant Vax2 is capable for inducing RGC axon growth *in vitro*. (A) E13.5 WT retinal explants were incubated in the presence and absence of Vax2-His (100 ng/ml) for 24 h. The explants were then fixed for immunostaining with rabbit anti-Vax2 antibody (green) and mouse anti-NF160 antibody (red). DAPI (blue), nuclear counter staining. Immunostaining images in the bottom panel are magnified versions of dotted boxed area in top panel. Arrow indicates Vax2-His proteins internalized to RGC axons. Scale bars are 500 μ m (top) and 100 μ m (bottom), respectively. (B) Dark field images of the explants were taken before (0 h) and after (24 h) incubation period. The

changes in axonal length during the 24-h incubation period were measured and compared with untreated control samples. The values in the graph are averages and error bars denote SDs. The scores on top of graph columns are the numbers of axons analyzed. Numbers of explants analyzed are: 6X-His, n=5; Vax1, n=4. *P*-values were determined by Student *t*-test (**, *p*<0.001).

Figure 4 – figure supplement 1. (A) Vax1 mRNA was detected in the HT, hypothalamic cell cord (HCC), and optic nerve (ON) approaching the OC of E14.5 WT (*Vax1*^{+/+}) embryonic brains (top left). Vax1 proteins, assessed by immunostaining with an anti-Vax1 antibody, were also detectable in these structures (top right). However, Vax1 immunostaining signals as well as Vax1 mRNA were absent in these structures in the brains of *Vax1*^{-/-} littermates (bottom). (B) Vax1 localization in E14.5 *Vax1*^{lacZ/+} mouse vHT cells, which also express β-gal from one Vax1 locus, was examined by co-immunostaining for Vax1 and β-gal. All cells that expressed β-gal also expressed Vax1 (arrowhead), but some Vax1-positive cells lacked β-gal (arrow). Vax1 was not detected in the brains of *Vax1*^{lacZ/lacZ} homozygous knock-in mice, which express β-gal from both Vax1 loci, confirming the specificity of Vax1 immunostaining. Scale bars: 50 μm

Figure 4 – figure supplement 2. Cytoplasmic localization of Vax1 in RGCs. Sections of E18.5 WT (top) or *Vax1*^{lacZ/lacZ} mouse retinas (bottom) were immunostained with rabbit α-Vax1 and gold (25 nm)-labeled anti-rabbit IgG, and analyzed by electron microscopy, as described in Figure 4D. Arrowheads in RGC images point to Vax1 proteins in the intracellular vesicle, whereas arrows in the images indicate Vax1 proteins bound to the extracellular surface of the RGC plasma membrane (top). Arrowheads indicate Vax1 proteins in trafficking vesicles, whereas arrows mark soluble Vax1 in the cytoplasm (bottom).

Figure 7 – figure supplement 1. Molecular determination of the interaction between Vax1 and Sdc. Vax1 (A) or Vax2 (B) was co-expressed with GFP-tagged Sdc1 and Sdc2 in HEK293T cells. GFP-fused Sdc1 and Sdc2 protein complexes were isolated by immunoprecipitation (IP), and Vax1 and Vax2 proteins in GFP-Sdc1 and GFP-Sdc2 immune complexes were detected by Western blotting using α-Vax1 (A) or α-Vax2 (B). (C) The Vax1-interacting domains of Sdc2 were examined by co-expressing Vax1 with Sdc2-

N, which lacks the cytoplasmic domain, or with Sdc2-C, which lacks the extracellular domain. GFP-Sdc-N or GFP-Sdc-C protein that co-immunoprecipitated with Vax1 was detected by Western blotting with α -GFP. Relative levels of Vax1, Vax2, and GFP-Sdc2 proteins in cell lysates (CL) used for IP were also examined by Western blotting (bottom two panels in A – C).

Figure 7 – figure supplement 2. (A) Co-localization of Vax1 and Sdc3 in RGC axons. Distribution of Vax1 and Sdc3 in E14.5 mouse embryonic eyes was examined by co-immunostaining with rabbit anti-Vax1 (green) and goat anti-Sdc3 (red) antibodies. Image in the third is a merged magnification of area marked by dotted boxes in left two images. Plots in the right column indicate fluorescence intensities of areas marked by dotted lines in the third. Arrowheads on plots indicate fluorescence intensities of the corresponding points in the images. N, nasal; T, temporal. Scale bars: 200 μ m (left two panel) and 20 μ m (third panel). (B) Retinal explants isolated from dorsal-temporal (DT) and ventral-temporal (VT) parts of E13.5 mouse retinas were treated with Vax1-His protein (100 ng/ml) for 24h. The explants were then fixed for immunostaining with rabbit anti-Vax1 (green), mouse anti-NF160 (red), and goat anti-Sdc3 (blue) antibodies. The localization of Vax1 and Sdc3 in NF160-positive RGC axons was examined by confocal microscopy (see details in Materials and methods). Scale bars: 500 μ m (left column) and 50 μ m (magnified images at right).

Figure 8 – figure supplement 1. Biophysical properties of Vax1(WF/SR) mutant protein. (A) Trp and Phe (WF) at amino acid residues 147 and 148 of mouse Vax1, which are homologous to critical residues of the cell-penetrating region of the Antp (antennapedia) homeodomain (Joliot et al, 1998), were mutated to Ser-Arg (SR) in Vax1(WF/SR). Vax1 and Vax1(WF/SR) interactions with GFP-Sdc2 were assessed by immunoprecipitating cell lysates with α -Vax1 and subsequent Western blotting with α -GFP. Successful expression of Vax1 and GFP-Sdc2 was also assessed by Western blotting of cell lysates. (B) COS7 cells were incubated for 3 h with growth medium (S3 fraction) from HEK293T cells overexpressing Vax1-V5 or Vax1(WF/SR)-V5. Vax1 protein at the intact cell surface was detected with rabbit α -Vax1 (green), whereas Vax1 protein inside cells and at the cell surface of fixed cells was labeled with mouse α -V5 (red). After incubating with Alexa 488-conjugated α -mouse IgG and Cy3-conjugated α -rabbit IgG, the distribution of cell surface

and intracellular Vax1 was analyzed by confocal microscopy. Scale bars: 20 μm . (C) The importance of cell penetration of Vax1 for RGC axonal growth was investigated by co-culturing mouse retinal explants (NR) with COS7 cells overexpressing WT Vax1 or Vax1(WF/SR) mutant for 48 h. The explants were then stained with rabbit α -Vax1 (green) and mouse α -NF160 (red). Scale bars: 500 μm (top) and 200 μm (bottom). (D) Relative axon content in each angle segment was analyzed as described in Methods and is shown graphically. The values in the graph are averages, and error bars denote standard deviations (SD). Results were obtained from three independent experiments. The scores under y-axis labels are the numbers of explants analyzed. *P*-values are between 0.001 and 0.005 (ANOVA).

Figure 9 – figure supplement 1. vHT-secreted Silt inhibits RGC axon growth. (A) E13.5 WT retinal explants were co-incubated with E13.5 *Vax1-ko* vHT explants for 24 h in the presence (bottom) or absence (top) of Robo1-Fc (100 ng/ml). Dark field images of the explants were taken before (0 h; left column) and after (24 h; center column) the incubation. The explants were then fixed for immunostaining with mouse anti-NF160 antibody (red). Immunostaining images of dotted boxed areas in center column are shown in right column. DAPI, nuclear counter staining. Scale bars denote 500 μm . (B) The angular distribution of RGC axons was measured by counting axon marker NF160 immunostaining image pixels (axon counts) as described in Materials and methods and presented graphically. +, forward direction angle segment; 0, neutral direction angle segments; -, reverse direction angle segment. The values in the bar are averages, and error bars denote SD. Numbers under y-axis labels are the numbers of explants analyzed. *p*-values determined by ANOVA test are <0.01.

Figure 9 – figure supplement 2. Reciprocal antagonism between Vax1 and Slit2 *in vitro*. (A) E13.5 mouse retinal explants were cultured for 24 h prior to treatment with Slit2-His (10 ng/ml; R&D Systems) for 24 h in the absence (left) of Vax1-His or in the presence of 10 ng/ml (middle) or 100 ng/ml (right) of Vax1-His (top row). In reciprocal experiments, explants were treated with Vax1-His (10 ng/ml) for 24 h in the absence (left) of Slit2-His or the presence of 10 ng/ml (middle) or 100 ng/ml (right) Slit2-His (bottom row). (B) The changes in RGC axon length during the last 24 h are shown graphically. Error bars denote SDs and the scores on top of graph columns are the numbers of axons analyzed.

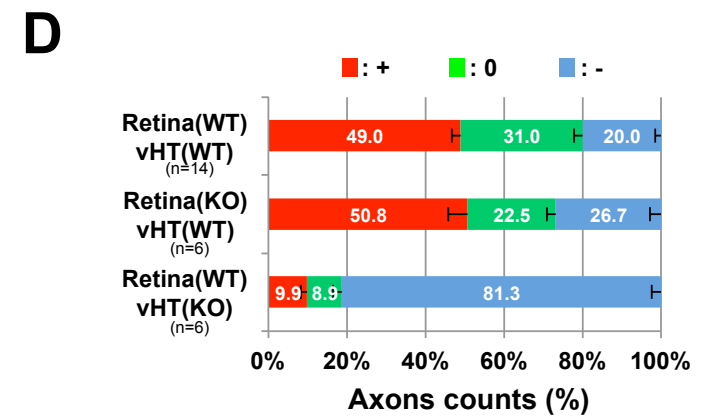
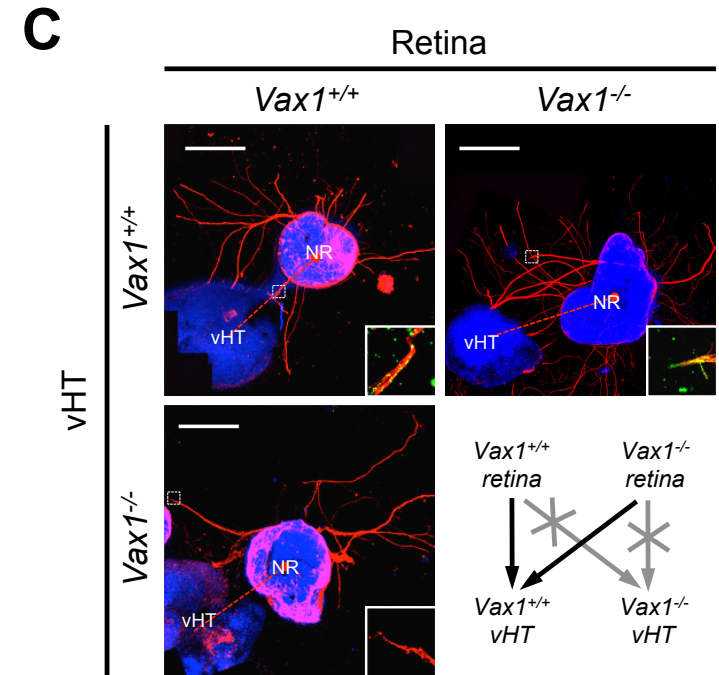
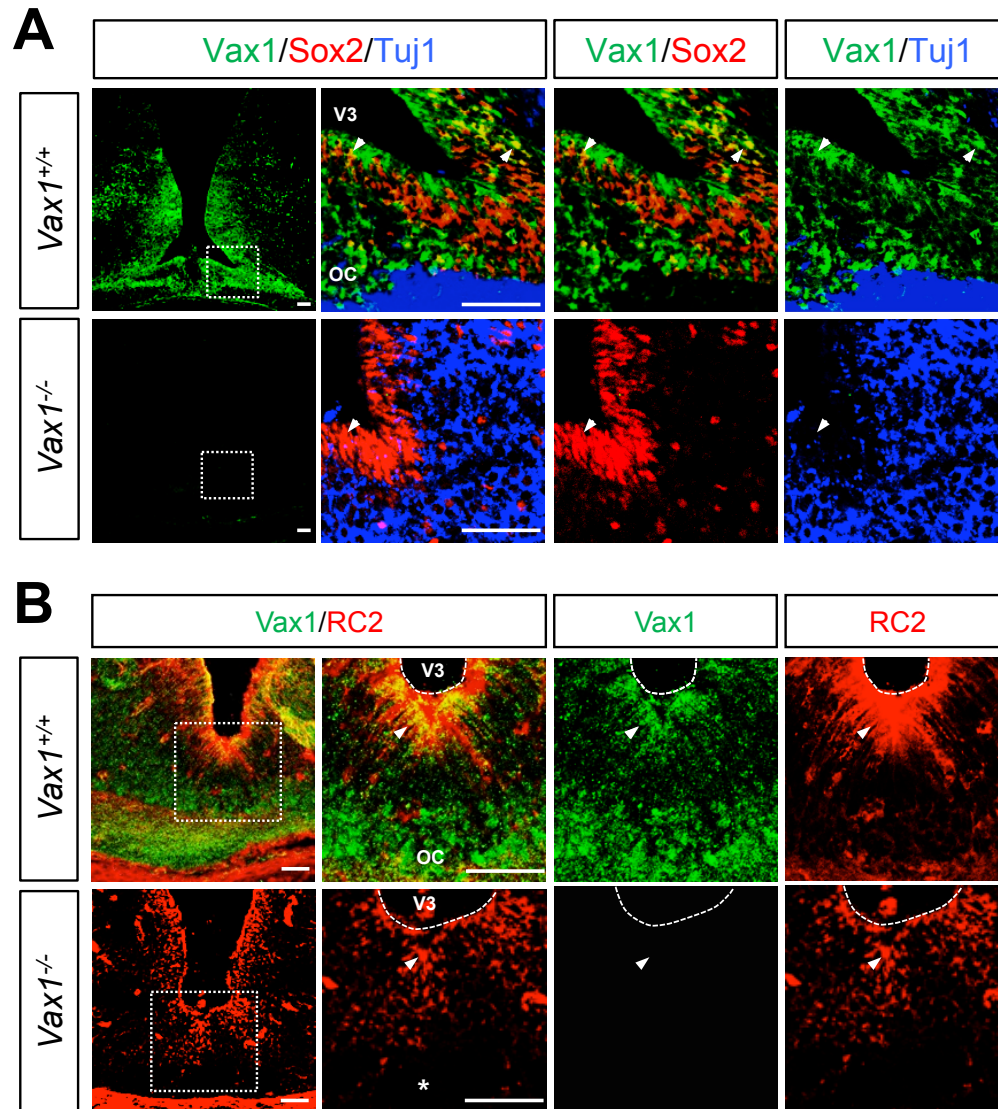
Numbers of explants analyzed: Untreated, n=22; Vax1 (10 ng/ml), n=10; Vax1 (100 ng/ml), n=9; Slit2 (10 ng/ml), n=5; Slit2 (100 ng/ml), n=5; Vax1 (10 ng/ml)+Slit2 (10 ng/ml), n=7; Vax1 (10 ng/ml)+Slit2 (100 ng/ml), n=6; Vax1 (10 ng/ml)+Slit2 (10 ng/ml), n=13; and Vax1 (100 ng/ml)+Slit2 (10 ng/ml), n=7. Results were obtained from four (for the first two) or three (for the rest) independent experiments. (C) Vax1-His and Slit2-His added to retinal explants were detected by immunostaining with rabbit α -Vax1 (green) and mouse α -Slit2 (red). Scale bars: 20 μ m. Fluorescent intensities Vax1 and Slit2 immunostaining images were measured by Image-J software and shown graphically. Scores on top of columns are numbers of areas analyzed. Numbers of explants analyzed for immunostainings are same as (B).

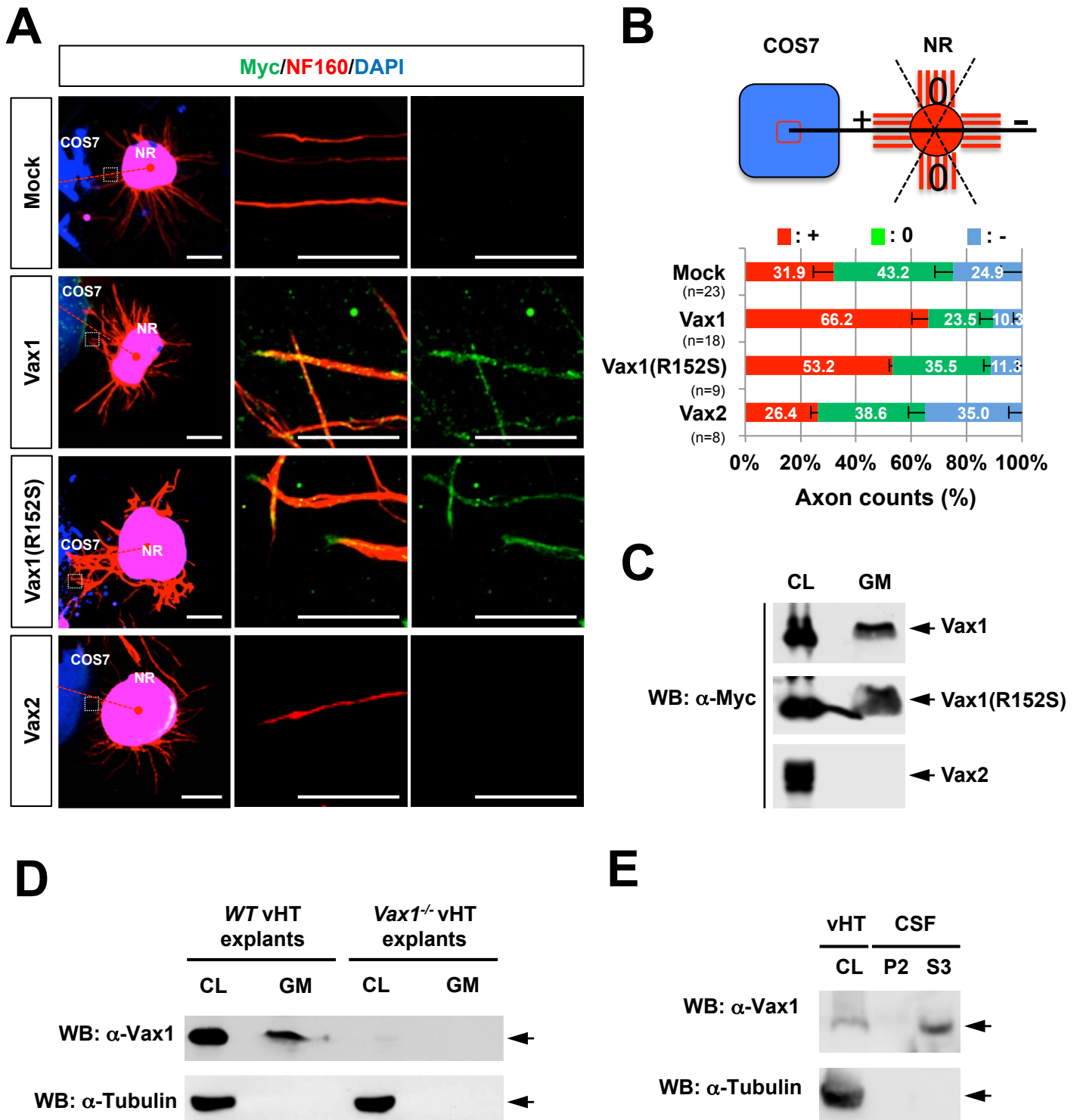
Video supplements

Video supplement 1. Time-lapse video of E13.5 mouse retinal explants cultured in the presence of 6X-His-FITC peptides (100 ng/ml) as described in Materials and Methods.

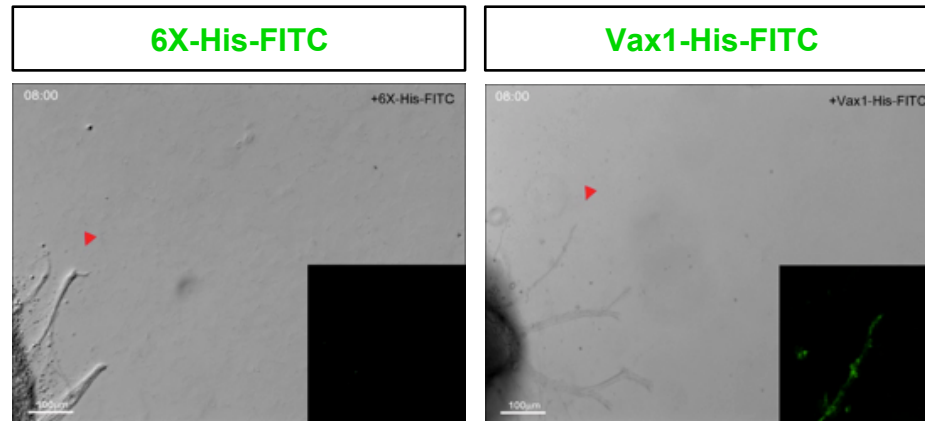
Video supplement 2. Time-lapse video of E13.5 mouse retinal explants cultured in the presence of Vax1-His-FITC proteins (500 ng/ml) as described in Materials and Methods.

Video supplement 3. Time-lapse video of E13.5 mouse retinal explants cultured in the presence of 6X-His-FITC peptides (500 ng/ml) as described in Materials and Methods.

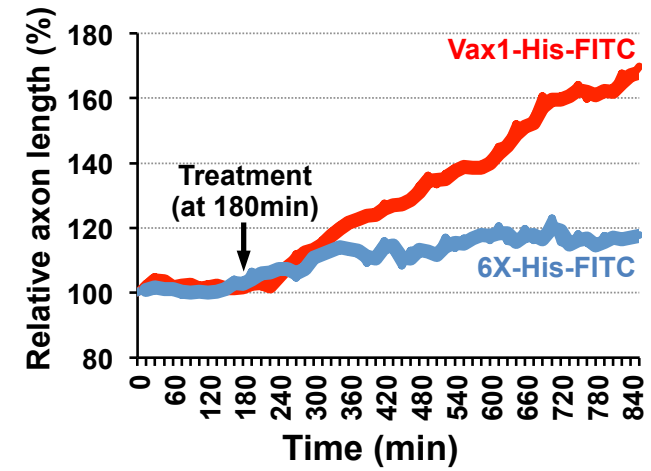




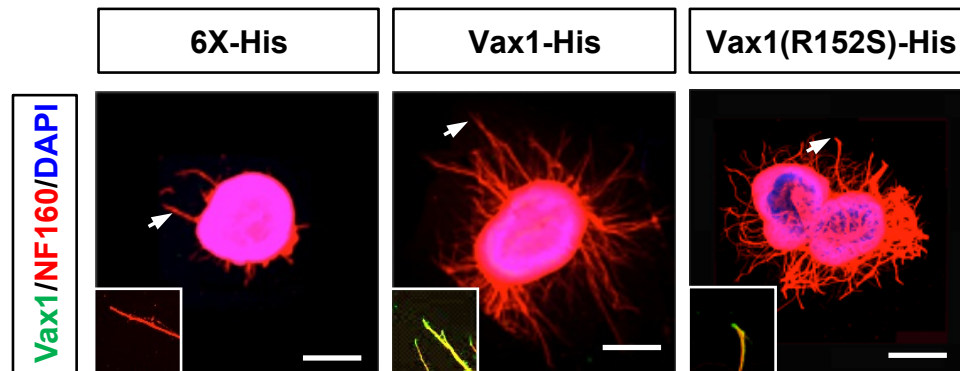
A



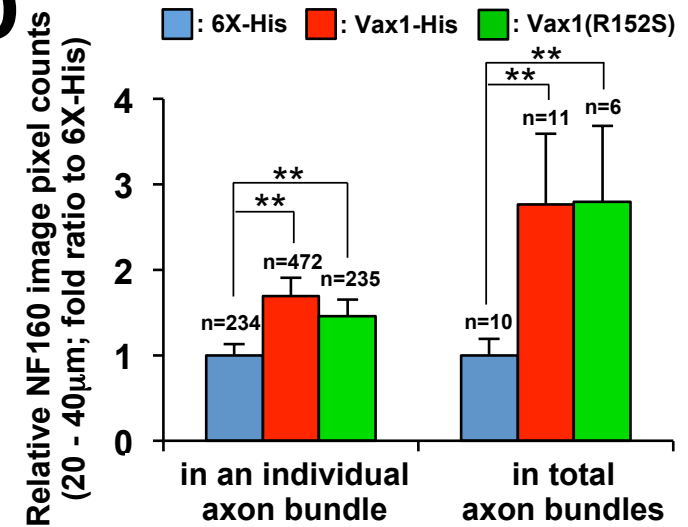
B

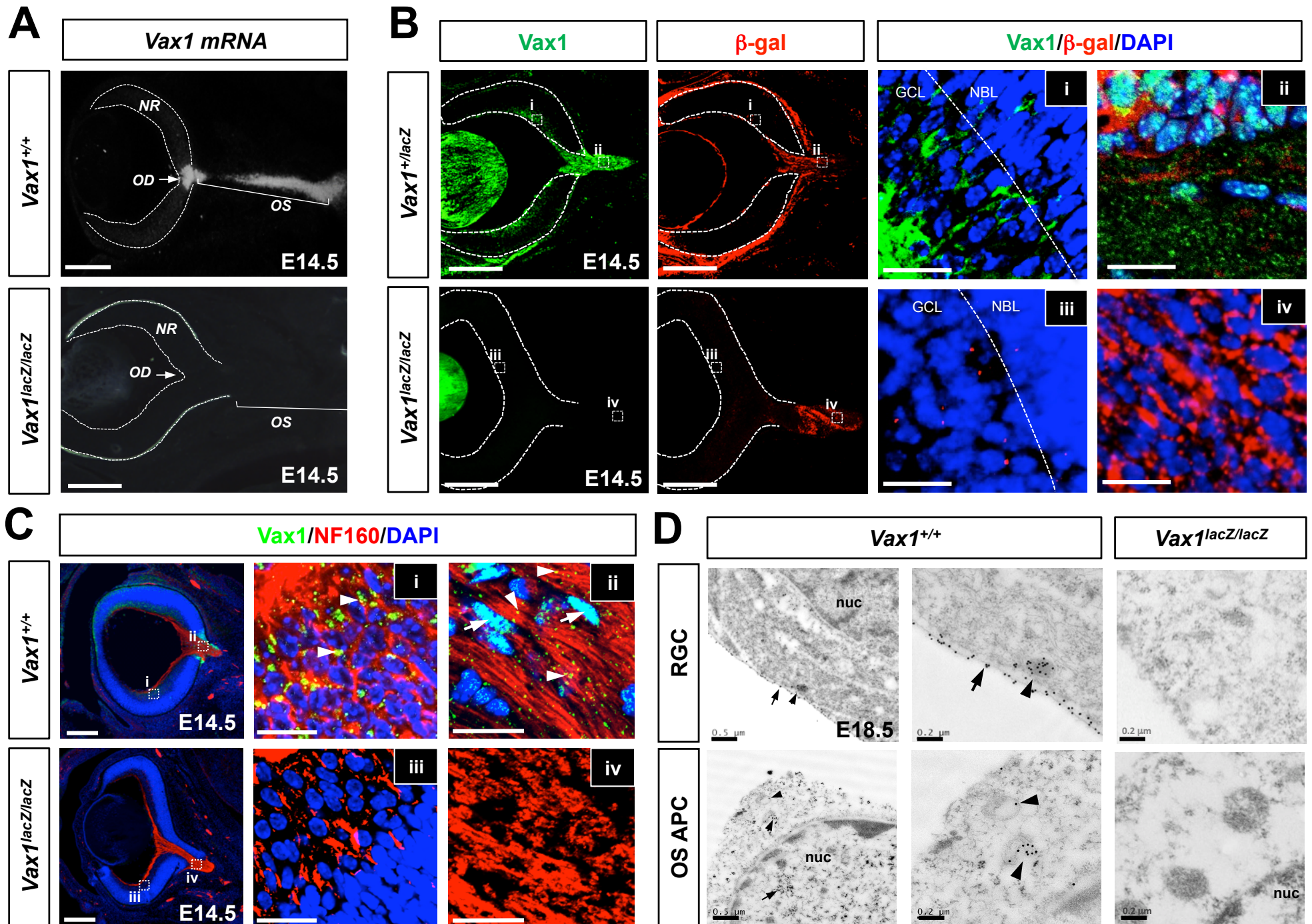


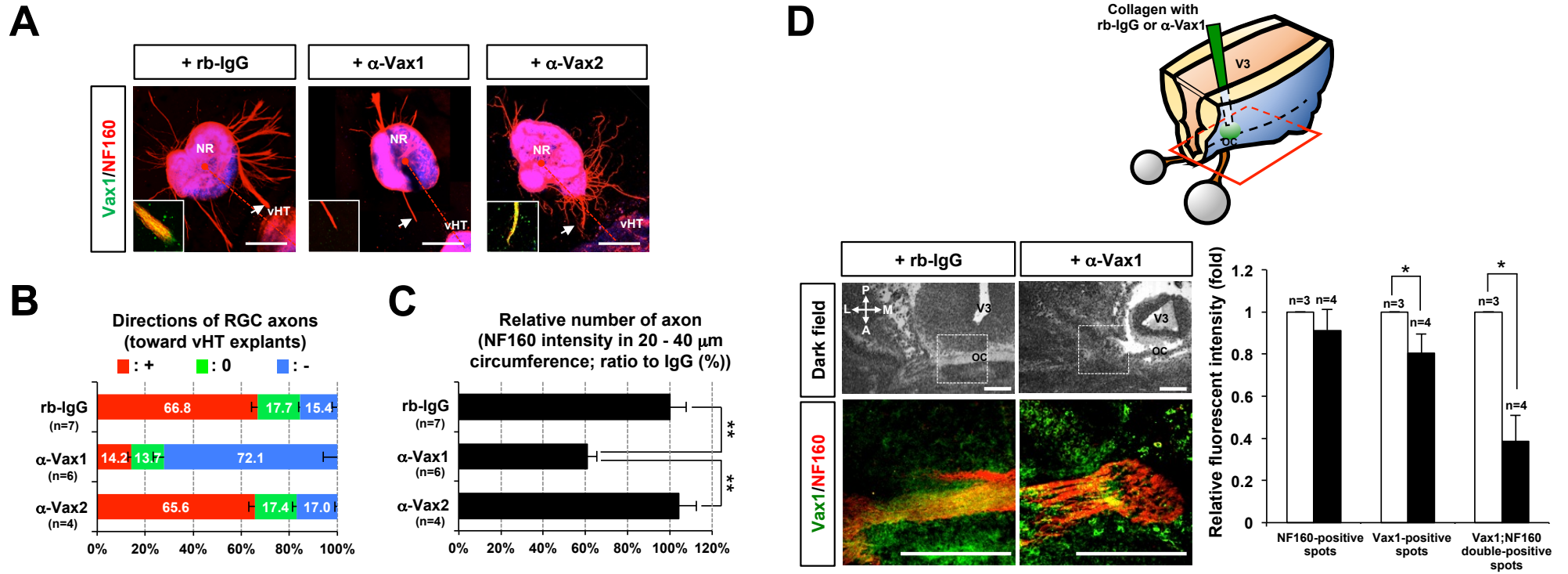
C

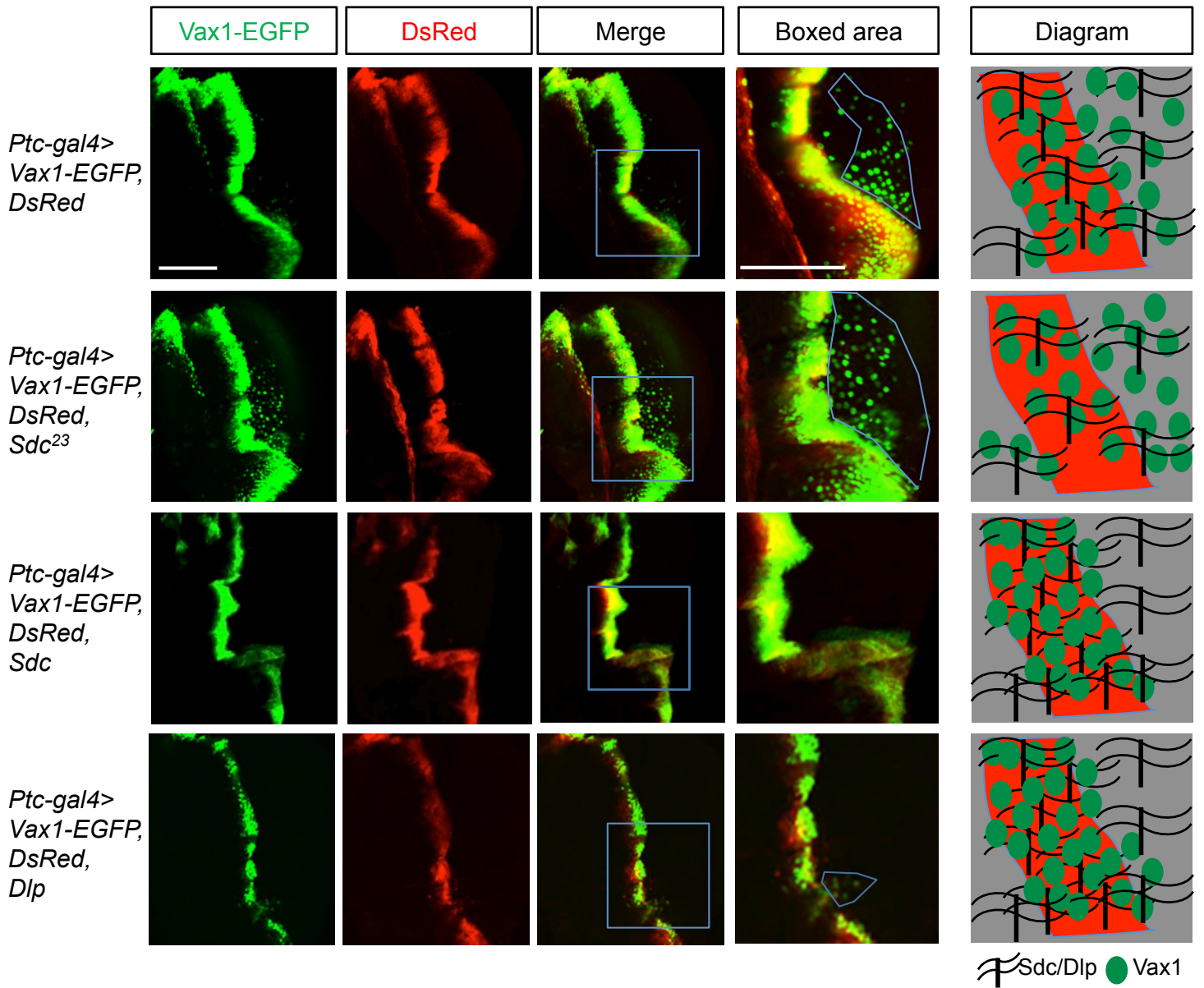


D

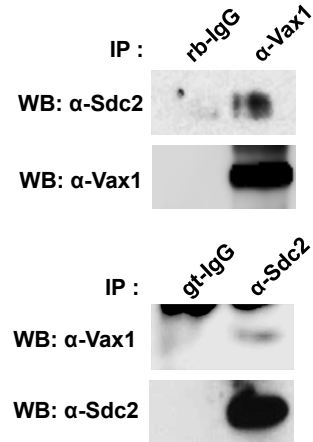




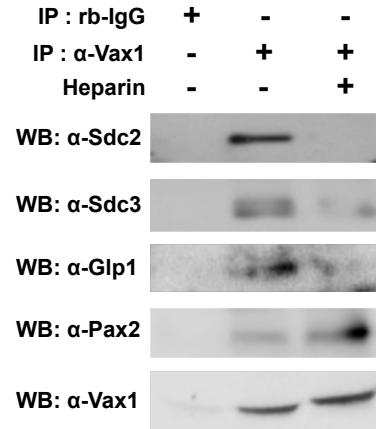




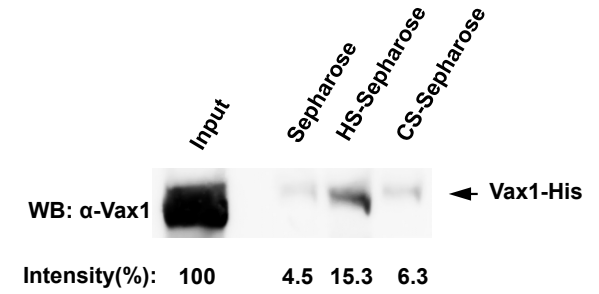
A



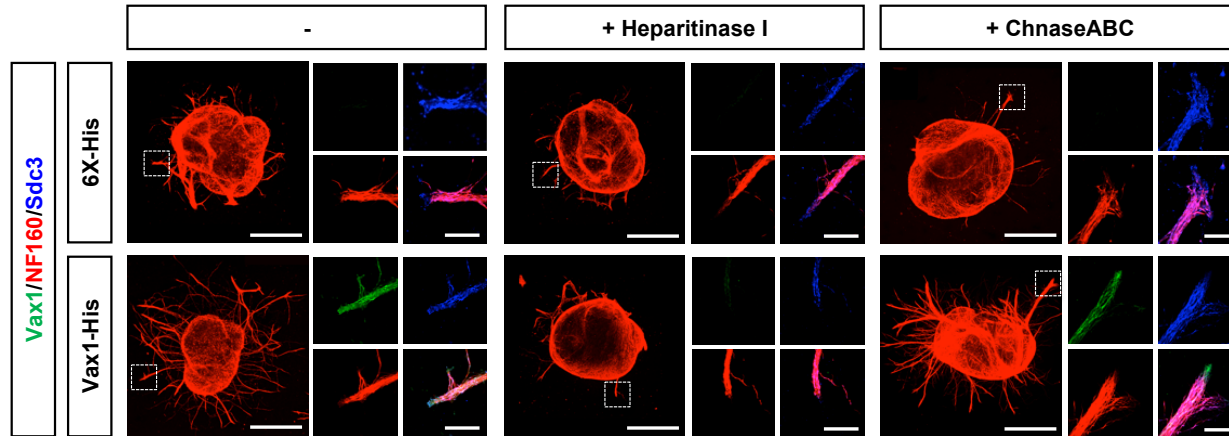
B



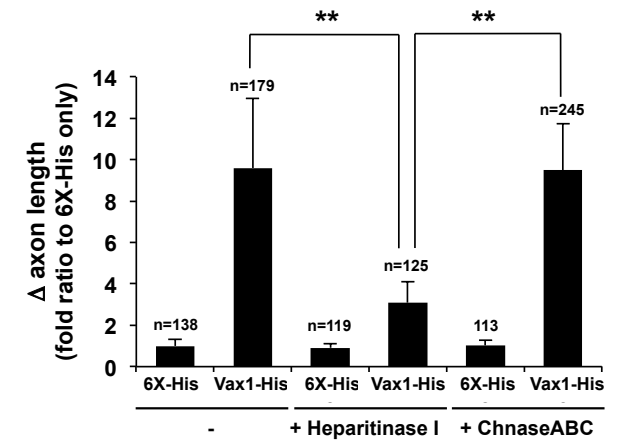
C

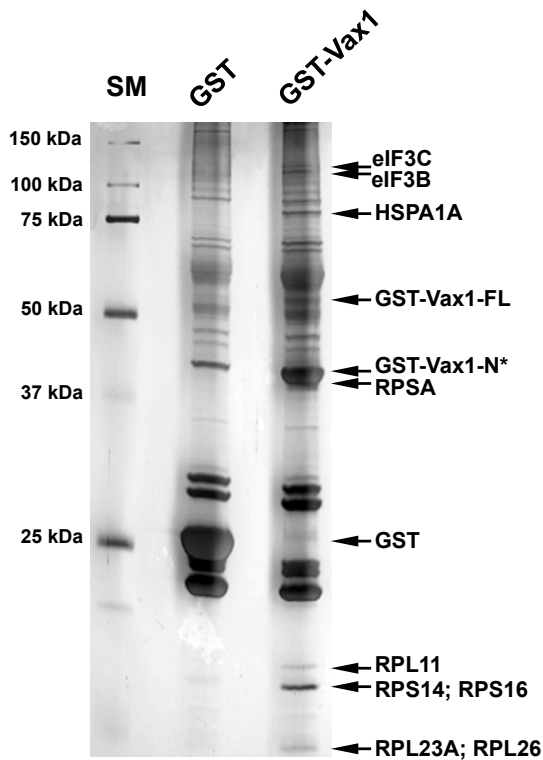
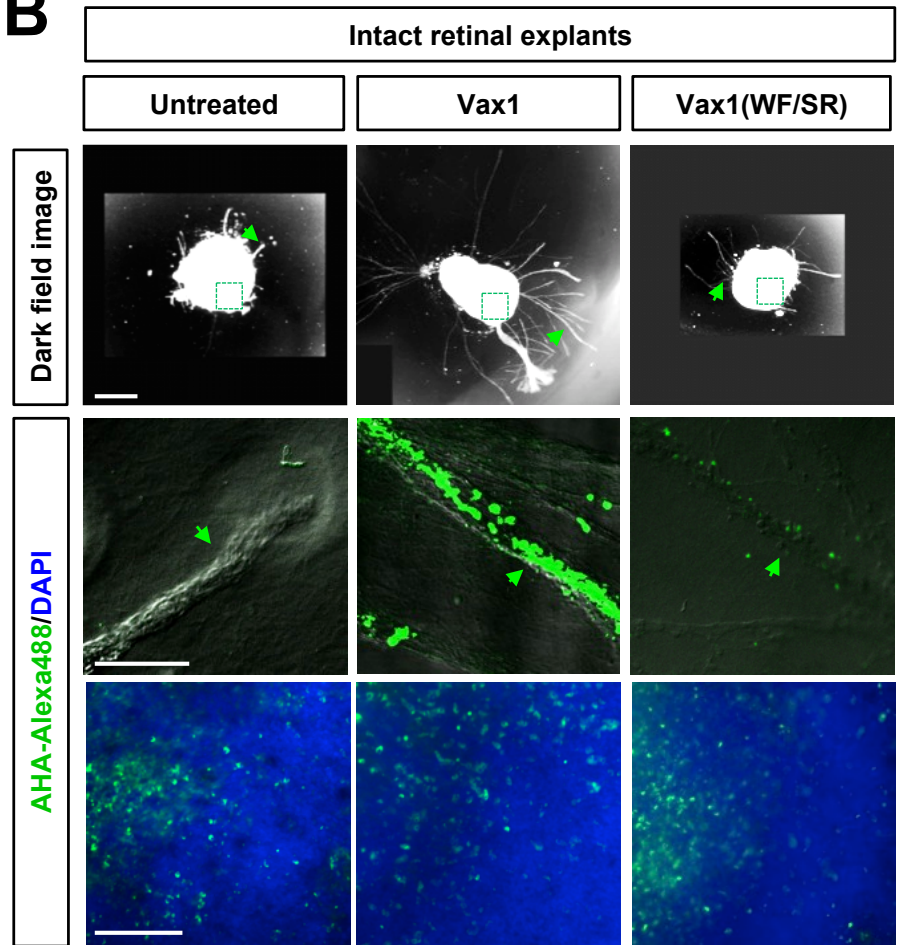
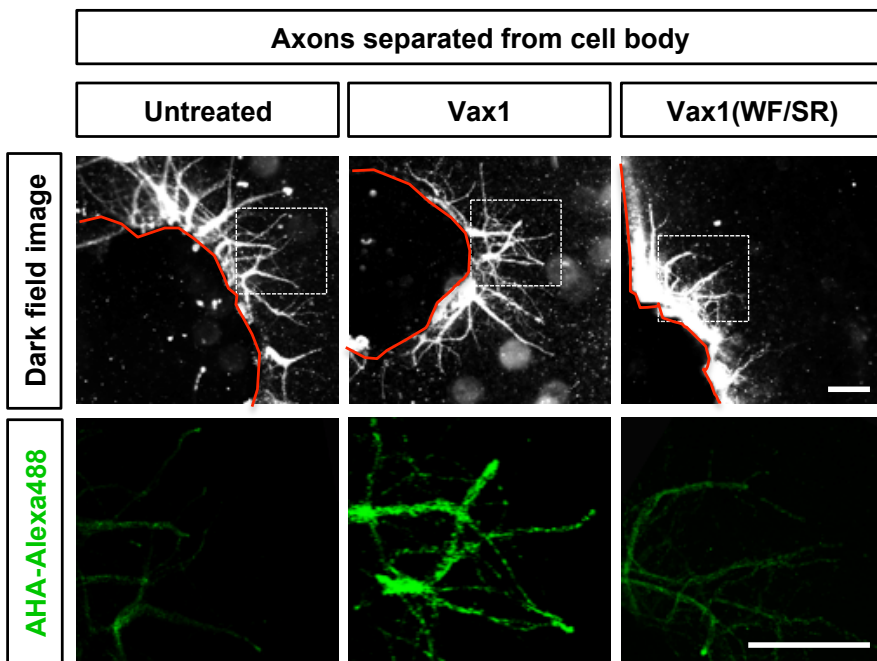
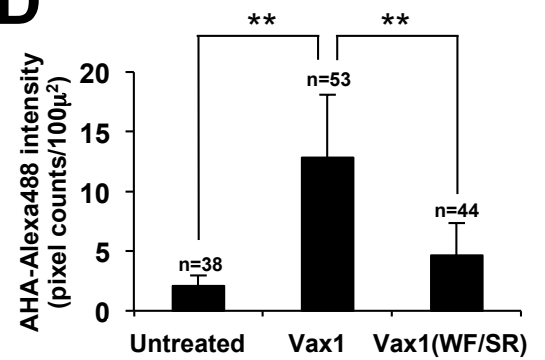
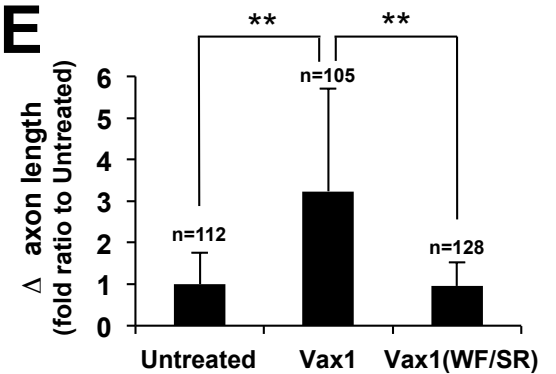


D

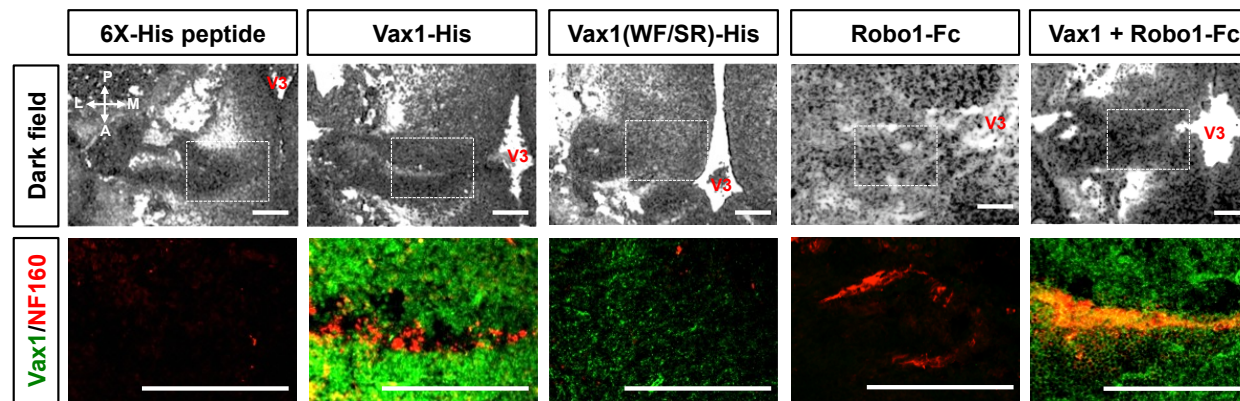


E



A**B****C****D****E**

A



B

